AN ABSTRACT OF THE THESIS OF

Kevin C. Womack for the degree of Doctor of Philosophy in Civil Engineering presented on June 6, 1989.

Title: The Dynamic Behavior of a Cable Logging Skyline and its Effect on the Tailspar

Abstract Approved: _____
Harold I. Laursen

Initially, a small experimental study was undertaken to examine the influence of incline on the frequency of taut cables. The experiments consisted of exciting a short cable at angles of incline from zero to 90 degrees and at various tensions. The results from these experiments shows a small effect due to the incline as the cable approaches the vertical. However, this influence is small enough that the theoretical equation for the frequencies of a horizontal cable could be used to determine the frequencies of a taut, inclined cable.

A computer model intended to simulate the dynamic behavior of a cable logging system skyline is the main thrust of this paper.

In developing the computer model both finite element and finite difference methods were considered. The finite difference method was selected based on its efficiency in

achieving the desired solution. A nine point implicit finite difference scheme, which guarantees stability of the solution, was employed.

Computer model output for skyline frequencies and tensions were compared with a number of field tests. The results were encouraging and indicated the model to be reliable in simulating the dynamic behavior of a skyline with a log load. This information can be used to determine the influence of dynamic skyline behavior on loads experienced by the tailspar.

The Dynamic Behavior of a Cable Logging Skyline and its Effect on the Tailspar

by

Kevin C. Womack

A THESIS

submitted to

Oregon State University

in partial fulfillment of
the requirements for the
degree of

Doctor of Philosophy

Completed June 6, 1989

Commencement June 1990

APPROVED:

_____

Professor of Civil Engineering in charge of major

_____

Head of Civil Engineering Department

_____

Dean of Graduate School

Date thesis is presented June 6, 1989

Typed by Kevin C. Womack

ACKNOWLEDGEMENTS

I would like to thank Dr. Marv Pyles for providing the funding on this project and Dr. Hal Laursen for being my major professor, working with him has been a great experience. Also I would like to express my sincerest appreciation to my wife, Dorothy, and children, Susana and Charles, for all they have sacrificed in allowing me to continue my education.

TABLE OF CONTENTS

LIST OF FIGURES

LIST OF FIGURES (cont.)

LIST OF TABLES

THE DYNAMIC BEHAVIOR OF A CABLE LOGGING SKYLINE AND ITS EFFECT ON THE TAILSPAR

INTRODUCTION

In the Pacific Northwest harvested logs must be moved from the spot where they are felled to a landing where they can be loaded onto trucks for transport out of the forest. The most commonly used apparatus for accomplishing this task on steep terrain is a cable logging system. Cable logging systems typically haul several logs up or down a hillside to the prepared landing. The major components of a cable logging system are: the yarder, which consists of several winches used to control the various cables and a vertical tower to assist in supporting these cables; the skyline, a cable that runs from the yarder to the end of the corridor being logged; the carriage, a mechanical device which rides on the skyline and from which a cable (dropline) is lowered that is tied around, or choked to, several logs; the mainline, which is used to reel in the carriage to the yarder; the haulback line, a cable that is used to pull the carriage back toward the tailspar (this line is not necessary for some types of carriages where gravity causes the carriage to return to the tailspar); and lastly, the tailspar which supports the tail end of the skyline (a tailspar may not be used depending on the terrain). An example of one type of cable logging system is shown in Figure 1, there are many other types of systems using some

or all of the components listed above in different configurations. The main components of interest in this project are the skyline, carriage, turn (load) of logs and the tailspar. The cables used in a cable logging system are wire rope which range in nominal diameter from 7/16 to 1 1/2 inches (11.1 to 38.1 mm), with span lengths ranging from 300 to 4000 feet (91.4 to 1216 m). A tailspar is a standing tree that has been topped (the upper portion of the tree removed) and is guyed, with two to four guylines, to provide additional stiffness. The purpose of the tailspar is to provide a support high enough so that the carriage is clear of the ground. At the tailspar the skyline passes through a large block hung near the top of the tailspar, and is tied off to a stump known as the tailhold. The carriage then rides on the skyline free of interference from the ground, though the logs being moved may still drag on the ground.

Interest in the tailspar, the loads placed on it and the resulting stresses it experiences during a typical yarding (retrieval of the logs) operation has been motivated by the change that has occurred in the forests. In past years logging has occurred in stands of trees that have been allowed to grow quite large, base diameters up to six or eight feet (1.83 to 2.44 m), over a significant period of time, up to hundreds of years. These stands of trees are known as old growth timber. When logging these areas it was simple to select a tree, that when guyed, would be more than satisfactory as a tailspar. However, in forests today, younger, smaller trees are more common

than the old growth timber. These stands of younger trees are known as second growth forests. The majority of timber harvested in the future will be second growth, which is intended to be harvested at ages from 40 to 100 years. Because of this the second growth timber is typically smaller than timber found in the old growth stands. In addition, the wood of a second growth tree is less dense than that of the old growth timber. The use of these smaller, weaker (due to the lower density of the wood) trees as tailspars, a typical tailspar in a second growth forest may be as little as 14 inches (0.36 m) in diameter at its base, gives rise to safety concerns about the ability of the tailspar to respond, without failure, to the loads placed it.

Extensive research has been done, and is currently underway, to examine the static response of a second growth tailspar to loads placed on it by the skyline and tailspar guylines. Included in this research have been studies of second growth tailspars that include a two-dimensional analysis of a tailspar as a beam column [1] and the development of a three-dimensional finite element model of a tailspar [2].

Research into the dynamic behavior of cable logging components has been less than that of static behavior. Only one study involving a tailspar has been found, a small experimental investigation into the frequencies of the tailspar guylines [3]. Another study of a cable logging system models the system as a two degree of freedom oscillatory system [4], but does not include a

tailspar.

The goal of this study was to investigate specifically the influence dynamic behavior of the skyline has on the loading experienced by the tailspar. The yarding cycle consists of several steps. The carriage, which starts at the landing, is moved along the skyline toward the tailspar until it reaches the desired position on the skyline. The mainline is given enough slack to allow the dropline (after going through the carriage the mainline becomes the dropline, it is the dropline that is choked around the turn of logs) to be pulled to the turn of logs. After placing the dropline around the turn of logs the logs are yarded in by pulling the carriage toward the yarder with the mainline. In some cases the turn of logs may not be directly under the skyline, and the logs will be first yarded transversely toward the skyline and then parallel to the skyline up to the yarder. At the yarder the turn of logs are placed on the landing and the dropline removed, then the cycle repeats itself. Within this yarding cycle a number of things can occur which will cause dynamic behavior of the skyline. One event which creates some of the highest tensions in the skyline, and through the dynamic behavior of the skyline results in large fluctuations of load on the tailspar, is the hang-up of the log load on some ground obstacle while the load is being yarded in. Often times this hang-up will stop the movement of the logs and the carriage, while the yarder operator will continue to reel in the mainline. This results in higher than normal tension in the skyline and

stored elastic energy throughout the system; when the hang-up breaks loose this initiates the dynamic behavior of the skyline with the resulting fluctuations of load on the tail spar. This event is what the computer model developed in this project is intended to model. By outputting the fluctuations in tension of the skyline, and the corresponding frequencies of the skyline, the dynamic response of the tailspar can be better determined.

Briefly, the computer program developed in this thesis to model the dynamic behavior of the skyline utilized a numerical approach in the form of a finite difference calculation of the nonlinear hyperbolic partial differential equation for a wave in a string, considering only displacements transverse to the string. This computer model will be useful in determining whether or not the dynamic loadings placed on a given tailspar by the skyline are critical. This type of information would be useful to loggers in the field who are concerned about their selection of a tailspar.

Verification of the computer model was accomplished by comparing output from the program to actual data collected in field experiments. A short skyline cable logging system, about 330 feet (100 m) in length, similar to the configuration of Figure 1 but without a tower, was erected in the Oregon State University research forest. This setup allowed for experimental work which yielded data that was used to confirm the computer model.

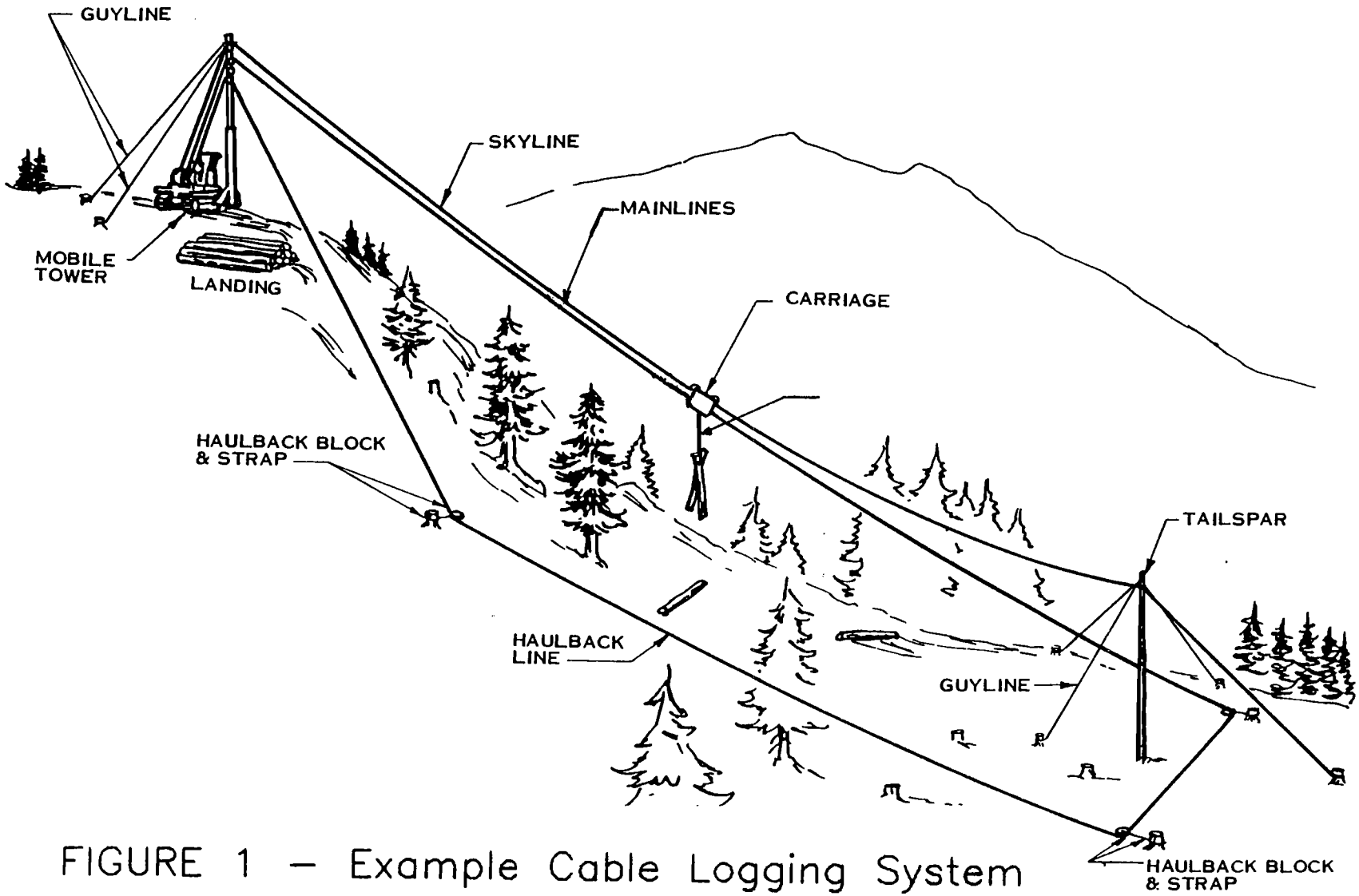

FIGURE 1 – Example Cable Logging System

CHAPTER 1 - Overview of Literature

The literature reviewed in preparing this thesis tended to concentrate on the determination of natural frequencies and mode shapes of cables in free vibration. Several methods of determining frequencies and mode shapes are set forth in literature, from a finite element type of approach [5,6] to analytical models of varying complexity [7,8,9]. The one major difference between the typical study of cable dynamics and the skyline dealt with in this study is the large point mass attached to the skyline in the form of the carriage, which is placed on the skyline, and the log load, which hangs from the carriage by way of the dropline. The problems created by this additional point mass, and the selection of finite differences as the method to model the cable behavior, are what gives this problem some of its unique characteristics and also takes it beyond the scope of most cable dynamics literature. In the structures area the use of finite differences to model the behavior of a cable is more often called a direct integration technique and is applied to the equation of motion (see Chapter 3, Equation 3) of a multi-degree of freedom system [10,11]. In applied mathematics the behavior of a cable is related to a wave in a string (wave equation, see Chapter 3, Equations 1 and 6), applying the finite difference method in this fashion is typically mentioned only in math texts [12].

During the review of available literature there were several points made that were applicable to this project.

It would be appropriate to mention these points here. A skyline in a cable logging system will have a certain amount of sag due to the weight of the cable. Several authors [7,8,11] point out that cables with a small sag to span ratio (sag being the maximum displacement of a cable segment from its chord) behave essentially as a taut (no sag) cable would and a parabolic profile of the cable is a good approximation to the profile of a cable under its own weight. A small sag to span ratio is generally considered to be less than 1:8, however, cables with sag to span ratios up to 1:4 or 1:5 are still considered to behave similarly to a taut cable.

The potential for several modes to be participating in the dynamic behavior of a skyline would certainly appear to be possible. Irvine [7] and Veletsos et al. [8] show in their writings that the antisymmetric modes (antisymmetric modes are more commonly called even modes, and are characterized by antisymmetric vertical displacements) create no overall change in the tension of a vibrating cable. This would indicate that only the symmetric modes (in most cases referred to as the odd modes, characterized by symmetric vertical displacements about the cable mid-point) would create a fluctuation in tension of a cable, while the antisymmetric modes would have no effect at all in the change in tension of the cable. For a skyline, with an evenly distributed mass and no large point mass, this means that any number of odd modes could contribute to the change in tension it might experience while in motion. However, when a large point

mass is attached to the skyline, the carriage and log load, it would seem that perhaps the fundamental mode would dominate, even though other odd modes could still participate.

Other basic principles of cable behavior are also mentioned in each of the above references. In many instances these basic principles are applicable to this study of the dynamics in a cable logging system skyline. When these principles are used they will be duly associated with the appropriate reference.

CHAPTER 2 - Frequency vs. Incline

In a cable logging system all of the cables involved, skyline, mainline, haulback line and guylines, are usually inclined at some angle. Very rarely would any of these cables be horizontal. The angle of incline of these cables could range up to 50 degrees.

The linear, free vibration equation of motion for a cable (wave equation) subject to its own weight and tension (no loads applied along the length of the cable and no variation in tension with time), with the end supports at the same level, is (for the derivation, see Appendix A):

$$T\frac{\partial^2 v(x,t)}{\partial x^2}=\rho\frac{\partial^2 v(x,t)}{\partial t^2} \qquad (1)$$

where T is the tension in the cable, ρ is the mass per foot of cable, x is the longitudinal axis, v is the displacement transverse to the cable and t is time. By solving this differential equation an expression for the frequencies of a cable can be obtained (see Appendix B):

$$f_n=\frac{n}{2L}\left(\frac{T}{\rho}\right)^{1/2} \qquad (2)$$

where f is the frequency in the n mode and L is the length of the cable. The point of interest with respect to the

analysis of cable logging systems was whether or not equation (2) could be used to calculate correctly the frequency of an inclined cable such as a skyline or a guyline. This would be useful in verifying parts of the computer model. Irvine's work [13] shows that equation (2) yields the best results when the sag to span ratio is less than 1:8, and acceptable results with a sag to span ratio up to 1:5. When considering guylines, or a tensioned skyline under its own weight, the sag is not a concern in that it easily meets Irvine's criteria for best results.

Several investigators have developed equations for calculating the frequency of an inclined cable [8,14] but these equations are quite lengthy and complicated. To simplify the analysis it was desireable to determine if equation (2) could be used directly, without modification, to accurately calculate the fundamental frequency of inclined cables, even up to the vertical position.

Experimental Investigation

Laboratory experiments were conducted in an attempt to support the use of equation (2) in calculating the frequencies of inclined cables. These experiments were conducted using a 7/16 inch (11.1 mm) diameter cable, 11 feet (3.35 m) in length, with a weight of 0.364 pounds/foot (5.31 N/m). The cable was a six-strand wire rope with an independent wire rope core, see Figure 2, typical of those used in cable logging systems. The

modulus of elasticity for wire rope is difficult to determine precisely. It is considered to range between 10,000 and 14,000 ksi (68.95 and 96.53 Gpa) [15] even though each wire is made of steel that has a modulus of elasticity of 29,000 ksi (200 Gpa). This lower modulus of elasticity for wire rope may be the result of several contributing factors. As seen in Figure 2, the individual wires are twisted in a strand to form a helix, and then the strands are twisted about a core to form another helix [16]. The angles of each helix, the change in these angles as load is applied to the cable and the fact that the individual wires are longer than the cable gage length all influence the modulus of elasticity [17]. In addition, the type of wire rope core, fiber or steel, and the friction that occurs between individual wires and strands also contribute to the modulus of elasticity of a wire rope. In the experiments, the cable was placed in positions ranging from horizontal to vertical, in increments of 10 degrees. At each position the cable was loaded to tensions of 500, 1000, 1500, 2000 pounds (2.22, 4.45, 6.67, 8.90 kN) and plucked to obtain a free vibration history. An example free vibration history, in the form of a damped sine wave, from one of these tests is shown in Figure 3. During the tests it was discovered that the end conditions were particularly critical. Any fixed-end type of rigidity at the ends was found to shorten the effective length of the cable and increase the

frequency. Because of this, the end conditions were designed to model pins as closely as possible. Accelerometers were attached to the cable at mid- and quarter-span points. These accelerometers were the easiest way of extracting the frequencies of the cable by examining the acceleration time histories. A power spectral density analysis, utilizing Fast Fourier Transforms (FFT) [18], was performed on the time history of each plucking test and the fundamental frequency extracted. This power spectral density analysis was available as a utility on the commercial data acquisition software that was used during these experiments [19].

Analysis

The frequencies calculated from equation (2) were then compared to the experimental frequencies. Figure 4 is a graph showing the ratio of the frequencies calculated by equation (2) to the experimental frequencies. These ratios are plotted against the angle of incline of the cable. A regression analysis was performed for the set of tests at each tension. The coefficient of determination, r^2, for regression of the frequency ratio on angle of incline ranged between 0.6 and 0.8 (all significant at $P<0.01$, where P is probability) [20]. The statistical significance of the regressions indicates that the frequency does change with incline; becoming lower as the cable is positioned near the vertical. This results in equation (2) yielding a higher frequency for cables at

inclines of 80 to 90 degrees.

It appears that as the cable is placed in a position close to, and including the vertical, a change in frequency results from the change in distribution of the weight along the cable (from normal to the cable to axial) and the change in direction of motion of the cable with respect to the weight distribution (from parallel to normal). This could be expected in a somewhat slack cable, where the weight of the cable is significant compared to the tension, but this investigation shows that this lowering of frequency also occurs in cables that are quite taut.

Even though the frequency does decrease as the cable approaches the vertical position, for the given cable and tension this change was slight. The error of equation (2) when compared to the experimental frequency was very consistent at both 80 and 90 degrees and was on the order of +4 percent. The results indicate that for short, small diameter cables, equation (2) can be used to calculate the fundamental frequency of a cable at any angle with an error range of ± 5 percent. Considering that a guyline or skyline would have a maximum angle of about 50 degrees, the results of this experimental work lends confidence to the use of equation (2) to calculate theoretical frequencies of guylines or skylines, without a large point mass, in order to verify the computer model.

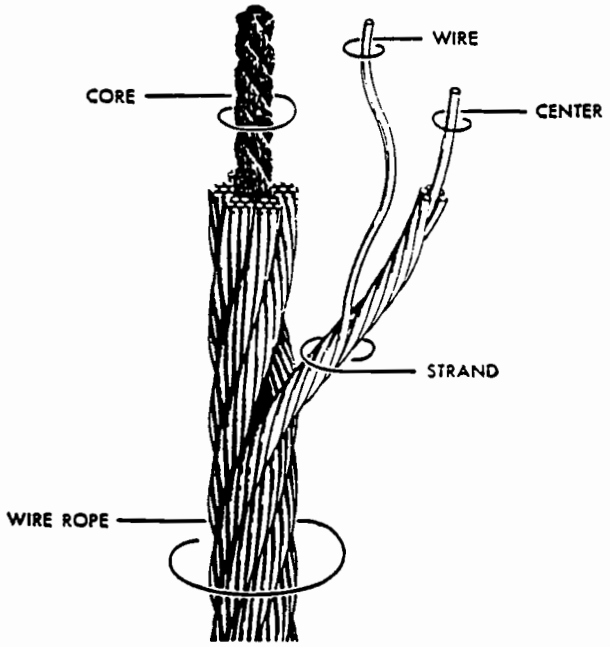

FIGURE 2 – Wire Rope Construction

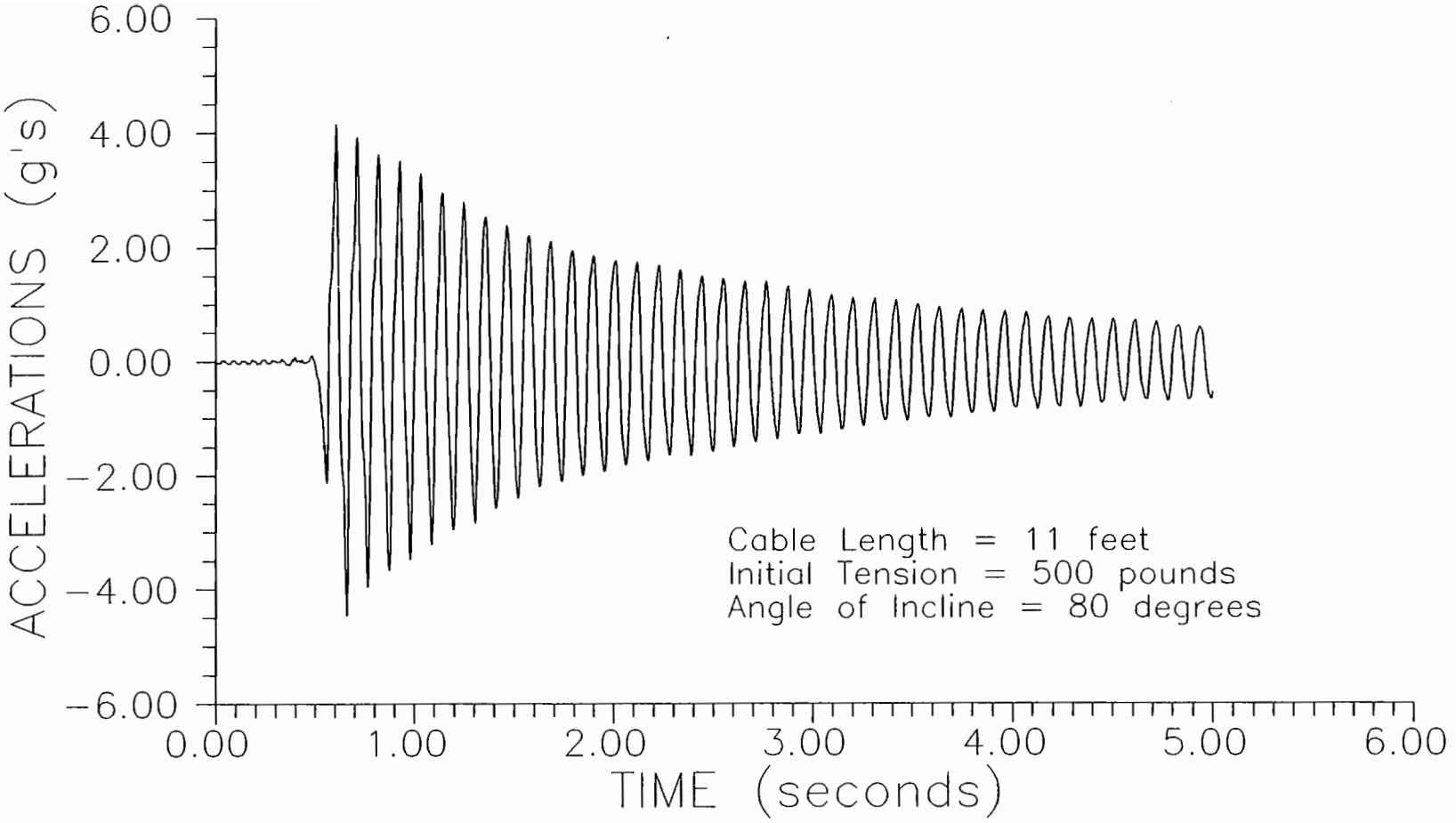

FIGURE 3 – Sample Acceleration Time History

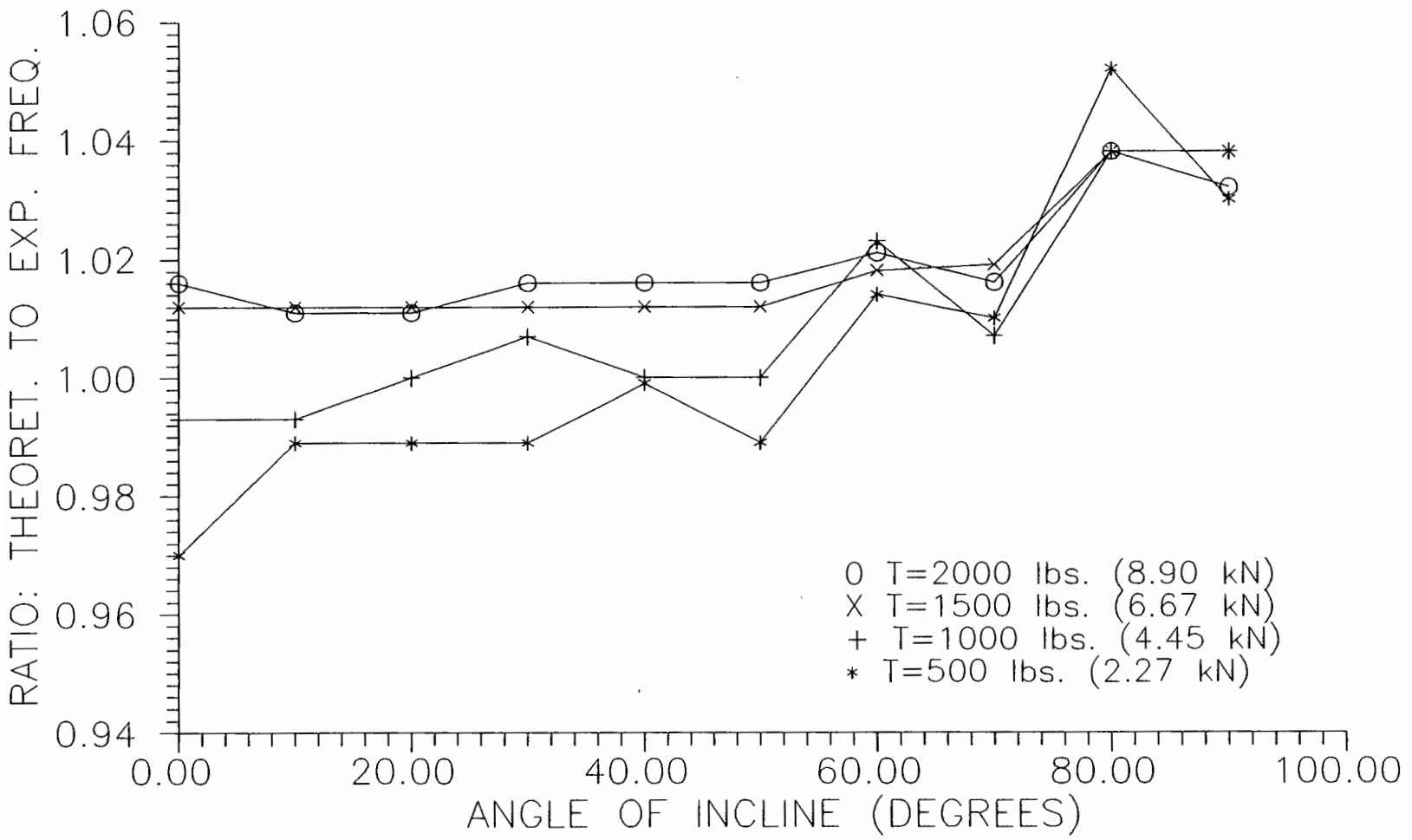

FIGURE 4
THEORETICAL FREQUENCY VS. EXPERIMENTAL

CHAPTER 3 - Finite Elements

The development of the computer model required the selection of a method to calculate the displacements of the cable. In the field of structural dynamics two options seemed to be most prominent:

1) Finite element method;
2) Finite difference method.

Given either method, the potential for large displacements of the skyline cable could result in geometric nonlinearities that should be considered in the solution.

This chapter contains a brief review and outline of steps that would be involved in the finite element approach to modeling the skyline. The next chapter will discuss the finite difference method.

In order to determine the displacements of a cable by the finite element method the cable is broken into a number of elements along its length. These elements are treated as a series of pin-connected truss elements that would constitute the cable. Though work has been done toward the development of a single element to model an entire cable [21,22], this strategy would not seem to be any more efficient than other finite element approaches because of the potential for participation of higher modes in cable oscillations. In order to account for these higher modes a single finite element would still require a number of lumped masses along its length, the result being a matrix solution similar to that of other finite element

strategies.

In order to determine the displacement time history of a cable, using the string of pin-connected truss elements, the finite element method involves a modal superposition analysis. The modal analysis approach utilizes the equation of motion for an undamped, multi-degree of freedom system:

$$[M]\{\ddot{D}\}+[K]\{D\}=\{0\} \tag{3}$$

to develop the eigenproblem, with the solution of the eigenproblem containing the natural frequencies of the cable (square root of the eigenvalues) and the mode shapes corresponding to the natural frequencies (eigenvectors). The mass matrix, [M], is a diagonal, lumped mass matrix. The stiffness matrix, [K], is a matrix of assembled individual truss element stiffness matrices. The vector, {D}, is the displacement vector. A modal matrix, $[\phi]$, is formed from the eigenvectors.

A second differential equation:

$$\ddot{Z}_n+\omega_n^2 Z_n=0 \tag{4}$$

is then solved to form the vector {Z}, which is the vector of modal amplitudes, where $\{D\} = [\phi]\{Z\}$; {D} and {Z} are both dependent on time. The natural frequencies are symbolized by ω. Considering the initial conditions and

the possibility that only a few of the lower natural frequencies, and corresponding modes, will participate the displacements of the cable, {D}, at a particular time are given by:

$$\{D\} = \sum_{n=1}^{m} (\phi)_n Z_n \tag{5}$$

For a linear solution this method is appropriate. However, in a nonlinear situation, which the skyline problem is, the modal analysis becomes more complicated due to the fact that the stiffness matrix, [K], is now a function of time also. The modification required by modal superposition is that at each time step the stiffness matrix, [K], is recalculated and is initially based on the displacements of the cable at the previous time step. This stiffness matrix is the "tangential" stiffness matrix for that time step. Convergence to the correct [K] and displacement solution at a given time is achieved through iterations of the displacement solution, see Figure 5. Popular iteration methods are the Newton-Raphson or modified Newton-Raphson approach. In the Newton-Raphson method the tangential stiffness matrix is updated at each time step, the modified Newton-Raphson method updates the tangential stiffness matrix less frequently. This is more efficient than constant updates, however, it may take more iterations for the modified method to converge to a solution.

This approach to the nonlinear problem is essentially a repeat of the entire linear solution at each time step with updates of the stiffness matrix due to the geometric nonlinearities and iterations to a correct solution. The eigenvalues and eigenvectors calculated at each time step are not the frequencies and mode shapes of the structure in the normal linear sense.

Although feasible, this approach becomes time consuming in reconstructing the necessary matrices at each time step. There is also the consideration of how well this technique converges to a correct solution. Cook et al. [10] states that the potential for poor convergence utilizing the modal superposition concept, especially for severe nonlinearities, is sufficient enough to merit consideration of other methods; he suggests direct time integration methods.

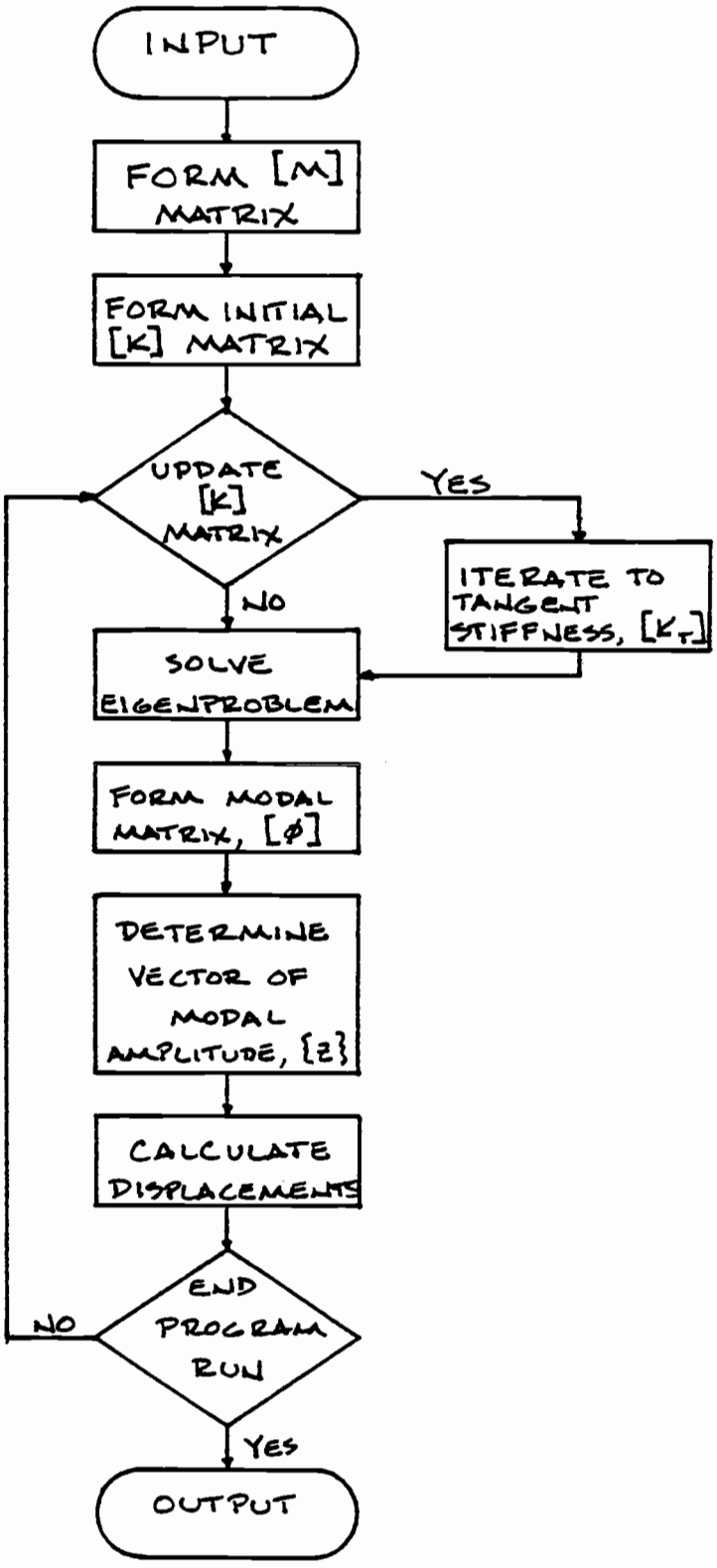

FIGURE 5
Finite Element Solution Flow Chart

CHAPTER 4 - Finite Differences

The direct integration methods Cook [10] refers to (see Chapter 3) are finite difference approximations. When considering the finite difference approach and its applicability to the skyline problem it was considered to be a way to model a wave in a string as opposed to a technique suitable for a multi-degree-of-freedom structural system. One may examine a cable logging system skyline either way and utilize the finite difference method to obtain a displacement time history of the cable in both cases. The finite difference concept deals with the wave equation more directly and efficiently than it would the multi-degree-of-freedom system. Even using finite differences the stiffness matrix, [K], would still need to be updated periodically and iterations performed to converge to a solution.

In finite difference terms, the cable has a series of nodes placed along its length. The relation of these nodes to each other is what is utilized in approximating the partial derivatives in the nonlinear equation of motion for a wave in a string, again for transverse displacements only. This differential equation is (for the derivation, see Appendix A):

$$\frac{\partial^2 v(x,t)}{\partial t^2} = \frac{T}{\rho}\left(\frac{\partial^2 v(x,t)}{\partial x^2}\right)\left(\frac{\cos\theta}{\sqrt{1+\left(\frac{\partial v(x,t)}{\partial x}\right)^2}}\right) \qquad (6)$$

θ is the angle of the tangent to the cable. The solution

of this differential equation gives the transverse displacements of points on the cable, which are a function of time and location on the cable and is given as v(x,t). In the solution the partial derivatives are approximated by divided differences. The first divided difference is simply the slope of a straight line connecting each of the nodes along the cable. The second divided difference, the one used to approximate a second derivative, is the difference of the first divided differences divided by the distance between the three adjacent nodes involved. Three points that need to be mentioned are: first, a uniform spacing between nodes may be used for convenience in programming. In certain instances a varying of the spacing between nodes can result in an increase in accuracy, but the result is also a more complicated program. Second, a partial derivative is approximated by taking the divided difference of one variable while the other is held constant. Third, the second divided difference is not a correct approximation of the second partial derivative. Due to the nature of the divided differences it is off by a factor of 1/2 if uniform time steps and spacing between nodes are used. The two divided difference tables pertinent to the wave equation are shown in Appendix C. Substituting these divided differences into the wave equation and rearranging the terms, the finite difference approximation of equation (6) becomes:

$$\frac{V_{ij-1}-2V_{ij}+V_{ij+1}}{(\Delta t)^2}=\frac{T}{\rho}\left(\frac{V_{i-1j}-2V_{ij}+V_{i+1j}}{(\Delta x)^2}\right)\left(\frac{\cos\theta}{\sqrt{1+\left(\frac{\partial v(x,t)}{\partial x}\right)^2}}\right) \quad (7)$$

The subscripts i and j indicate the node along the cable and the time step, respectively. As may be noted, the divided differences are functions of the displacements of an array of nodes with one unknown displacement at time j+1. This unknown displacement is determined for all nodes and the next time step is made, the j+1 and j displacement values become the j and j-1 values, respectively, and the j+1 displacement is determined, again for all nodes, from the two previous time steps, j and j-1. The cycle then repeats itself until the desired stopping time is reached. One way to visualize the operation of the finite difference model is to take a grid with the nodal positions across the bottom of the grid and the time steps along the side of the grid. The grid points themselves are the displacements of the nodes, v(x,t). Each side of the grid is a boundary, usually for which the displacements are known (typically zero). The finite difference model begins with the initial conditions, which are the first two rows of the grid, to calculate the displacement of the first node in the third row (actually the first time step). The model proceeds across the row, calculating the displacements at each node, and then jumps to the next time step. The finite difference method proceeds in this manner until the end of

the time history is reached. A three-dimensional view of this grid is shown in Figure 6. Note that no iterations or recalculation of matrices is required, even for the nonlinear case. If matrices are used the displacements at the latest time step simply replace a previous column in the matrix.

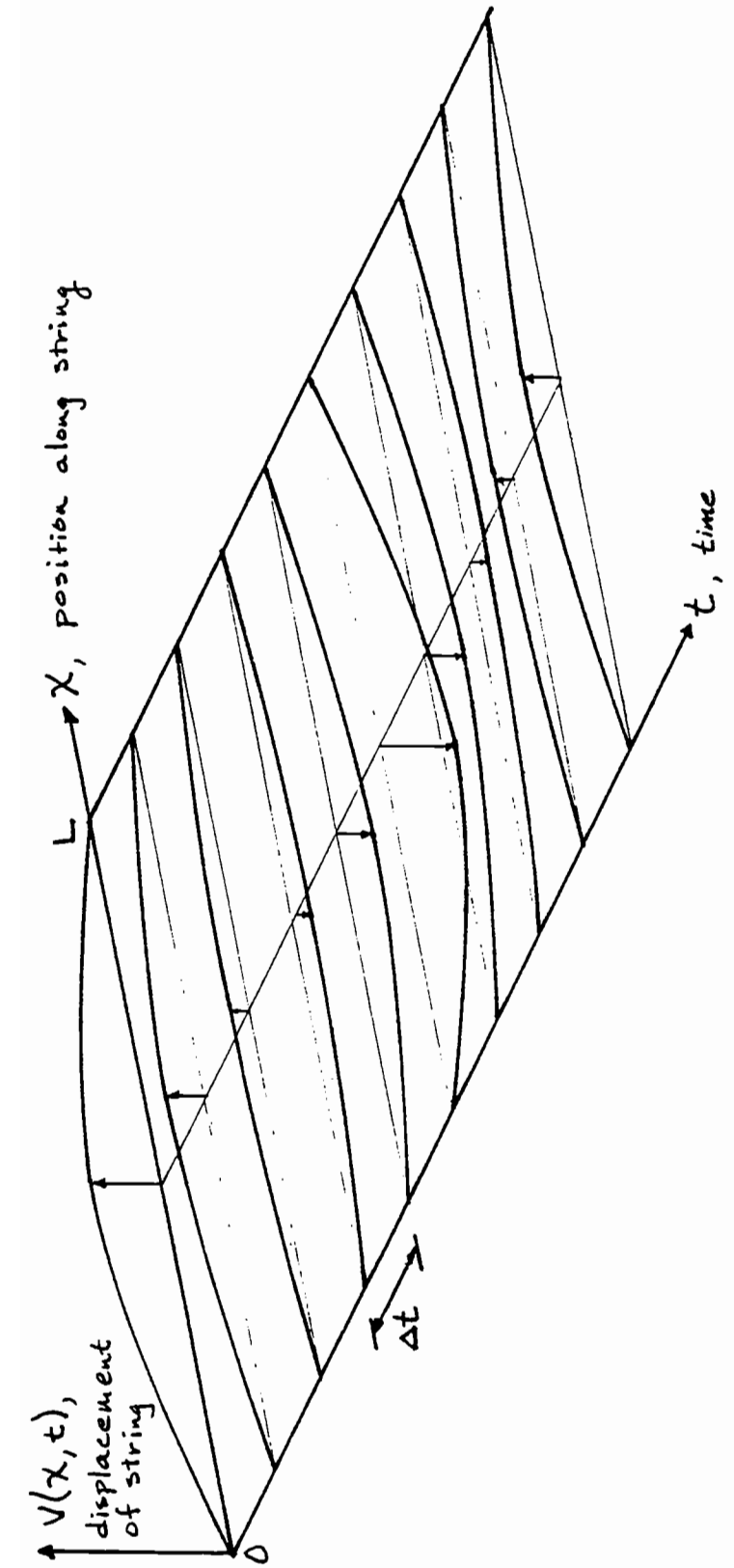

FIGURE 6
VISUAL OF FINITE DIFFERENCE SOLUTION

CHAPTER 5 - Modeling Considerations

Given the characteristics and efficiencies of the two methods discussed in the previous chapters, it was decided to utilize the finite difference model of a wave in a string. Following this decision some key characteristics of the skyline problem were addressed:

1) Initial conditions;
2) Boundary conditions;
3) Large point mass;
4) Array of finite difference grid points to be used in approximating the wave equation;
5) Skyline tension calculations;
6) Damping;
7) Inclination of the skyline.

Initial Conditions

The weight of the cable, carriage and turn of logs create an initial displacement and tension in the skyline. The profile of a cable displaced by its own weight is a catenary. Additional point loads would modify this catenary configuration. In order to simplify the determination of the initial skyline displacement it is desireable to utilize a parabolic approximation of the catenary profile and superimpose on that profile the deflection due to the point load of the carriage and turn of logs. As mentioned in Chapter 1, the profile of a simple cable with a sag to span ratio of less than 1:8 may be well approximated by a parabolic profile. In addition,

Irvine [7] introduces a dimensionless parameter Λ^2, which is an indication of cable stiffness due to geometric and elastic effects,

$$\Lambda^2=\left(\frac{\rho l}{H}\right)^2\left(\frac{1}{\left(\frac{HL_e}{EA}\right)}\right) \tag{8}$$

where l is the span of the cable, H is the horizontal component of cable tension, L_e is the actual length of the cable, E is the modulus of elasticity and A is the cross-sectional area of the cable. Irvine shows that if Λ^2 is less than 24 the cable exhibits taut string behavior. It seems to follow then that for a simple cable with a sag to span ratio of less than 1:8 (0.125) and Λ^2 less than 24, that a parabolic profile with superimposed point loads is an appropriate approximation to the actual configuration of the cable.

Figures 7 through 10 show values for sag to span ratios and Λ^2 plotted against skyline tensions for some simple cables with supports at the same level and with spans and tensions that would be encountered in skylines typical of cable logging systems before placement of a carriage and log load on the skyline. The tensions (percent of safe working load) are kept low for a skyline without a load so that a large load (carriage and turn of logs) may be placed on the skyline without exceeding the safe working load of the skyline. Sag to span and Λ^2 are independent of cable incline for parabolic approximations

if the span is considered to be the horizontal projection of the cable chord and the horizontal distribution of load is modified to account for the incline of the cable. These graphs indicate that skylines for many cable logging systems would meet the necessary taut cable criteria for the sag to span ratio which allows the initial displacement of the skyline to be calculated by the superposition of point loads on a parabolic profile. However, in all cases except a span of 1000 feet (305 m) or less with an initial simple cable tension of 25 percent or more of safe working load these skyline configurations do not meet the Λ^2 criteria for a taut cable. This indicates that linear superposition to determine the initial displacement of a skyline is not valid for most skyline configurations and that this use of linear superposition, which the model developed in this program utilizes, should be limited to skyline spans of 1000 feet (305 m) or less with an initial simple cable tension of 25 percent or more of safe working load. The initial displacement of a skyline which does not meet the sag to span or Λ^2 criteria that would allow linear superposition, would be correctly described by a catenary with a simultaneous (not superimposed) point load.

Initial tensions of the skyline are calculated based on the initial displacements of the skyline.

Boundary Conditions

The boundary conditions of the skyline, yarder and

tailspar, were treated as pinned supports. At both the yarder and tailspar the skyline usually passes through blocks which are attached to the tailspar and to a tower at the yarder end (see Introduction, Figure 1). After passing through these blocks the skyline is choked to a stump at the tailspar end and wrapped around a large reel at the yarder. The flexibility of the true boundary conditions would be difficult to determine and would vary for each tailspar and yarder. The number, and tension, of guylines for both the tailspar and yarder, the sway allowed by the blocks and the stiffness of the tailspar and yarder tower would all influence the flexibility of the boundaries. The treatment of the boundaries as pinned supports uncouples the skyline dynamic problem from the flexibility of the supports, initially reducing the complexity of the problem and allowing a simpler model to be developed. The results of this computer model, based on pinned boundary conditions, indicates whether or not further consideration of the supports is necessary.

Point Mass

The large point mass, carriage and turn of logs, breaks the skyline into two parts. The acceleration of this mass, due to the release of stored elastic energy, is also the driving force behind the dynamics of the skyline in a hang-up/breakout situation. It is considered as a moving boundary condition common to two cable segments. This treatment requires the calculation of the

displacement of the point mass and then the calculation of the displacements of the two individual cable segments.

Tychonoff and Samarski [23] derive an equation for the equilibrium of a point mass on a cable. By modifying this derivation to include the weight of the mass an equation of motion for the large point mass of the skyline problem was developed (see Appendix D). The true acceleration of the point mass, which is equal in magnitude but opposite in direction to the acceleration causing the inertial force, is represented by divided differences, resulting in the displacement of the point mass at the j+1 time step being represented in terms of time j and j-1 displacements. Once the time j+1 displacement is determined this becomes the new position of the common boundary and the displacements for the two cable segments are then calculated for the j+1 time step.

Labeling the carriage and turn of logs in a cable logging system as a point mass is a misnomer. The turn of logs is suspended from the carriage, which rides on the skyline, by the dropline allowing the turn of logs a certain amount of motion independent of the movement of the carriage. However, despite this inherent complication of the cable logging system, the mass and acceleration (transverse to the skyline) of the turn of logs has the same inertial effect on the skyline as an equivalent mass placed directly on the skyline would have. Therefore, in the computer model the mass of the turn of logs is treated

as if it were placed on the skyline and is added directly to the mass of the carriage.

Point Array

The array of points used in equation (6) is a five point scheme and is illustrated in Figure 11. This is perhaps the most common scheme because it comes directly from the divided difference tables. But there are also other arrays that may be used. The only prerequisite for an array is that it contain at least one displacement, which is to be determined, at the j+1 time step and known displacements from the j and j-1 time steps. Two other five point schemes are shown in Figures 12 and 13, with their corresponding equations for the wave equation. The fourth array, shown in Figure 14, is known as the nine point scheme and is a weighted average of the first three arrays, with the first five point scheme given a weighting twice that of the other two schemes.

Each scheme has its advantages and disadvantages. The first two schemes are explicit methods, meaning one unknown at the j+1 time is expressed, and solved for, in terms of known values at the two preceding time steps. Both of these procedures are easily programmed but a drawback is that both can have stability problems. To ensure that stability problems do not arise the multiplier in equation (7), known as λ,

$$\lambda=\left(\frac{(\Delta t)^2}{(\Delta x)^2}\right)\left(\frac{T}{\rho}\right) \tag{9}$$

must be less than or equal to one (see Appendix E). If this is not the case then the characteristics of the partial differential equation (domain of dependence) is not within the domain of the finite difference solution, resulting in an incorrect (rapidly unstable) solution. The characteristics of the partial differential equation must be within the domain of the finite difference solution [24]. By adjusting the size of time step and distance between nodes stability can be guaranteed, but for accuracy the spacing of nodes should not be too large and this can result in very small time steps being required for stability. If time steps are too small computing time can become quite long, certainly an undesirable situation.

The second two schemes are implicit and stable for all values of λ. Two or more unknown values at the j+1 time step are expressed, and solved for, in terms of known values from the two previous time steps. The stability of these procedures comes from the domain of the finite difference solution being the entire region of the grid up to and including the j+1 time step. The disadvantage of these two schemes is that there are three unknowns (displacements at the i-1, i and i+1 nodes) for a single array providing only one equation. This dilemma is resolved by taking the equations for each array across the j+1 row and developing a system of equations that would have m-2 unknown displacements (m being the number of

nodes including the boundary nodes for which the displacements are known) and m-2 equations. A more sophisticated program is required to use these schemes in the sense that a routine to solve systems of equations must be provided, but that is a minor detail due to the many efficient algorithms available. The stability of the implicit methods by far outweighs any disadvantages that might arise, reasonable sized time steps may be used in order to cut down on computing time. Of the two options, the nine point averaging scheme was selected for the computer model. Using a shorthand notation of the type:

$$\delta^2_{\Delta x} V_{i,j} = V_{i-1,j} - 2V_{i,j} + V_{i+1,j} \tag{10}$$

the finite difference equation for the nine point scheme is:

$$\delta^2_{\Delta t} V_{i,j} = \frac{T(\Delta t)^2}{\rho(\Delta x)^2}\left(\frac{\delta^2_{\Delta x} V_{i,j-1} + 2\delta^2_{\Delta x} V_{i,j} + \delta^2_{\Delta x} V_{i,j+1}}{4} \right)\left(\frac{\cos\theta}{\sqrt{1+\left(\frac{\partial v(x,t)}{\partial x}\right)^2}} \right) \tag{11}$$

Having selected the nine point scheme a routine for solving systems of equations was selected. Two methods were considered:

1) Lower Triangular/Upper Triangular Matrix Decomposition;
2) Gauss Elimination.

A characteristic of the system of equations developed from the nine point scheme is that the square coefficient

matrix is tri-diagonal. There are special Lower Triangular/Upper Triangular (LU) decomposition routines written for tri-diagonal matrices [25]. An algorithm for Gauss elimination involving a tri-diagonal matrix is not difficult either, so ease of programming was not a consideration. The selection of a method was based on the number of calculations and storage required to perform the operations. Analysis of each method shows that 5m multiplication and division operations are necessary for either method, given an m x m matrix. The storage requirements also ended up being the same for both methods. The tri-diagonal matrix can be stored along with the two vectors in a 5 x m rectangular matrix. Therefore, the selection of either method is simply up to personal preference. The Gauss elimination scheme was used in this project.

Skyline Tensions

Typical output for a dynamic time history analysis of a cable is the displacement at each node, but for this project the fluctuations in skyline tension (range or envelope of skyline tensions from maximum to minimum values) as the skyline oscillates and frequency of these oscillations are more important than displacement output. Knowing the displacements of the cable, a method of extracting the cable tension needed to be developed. The cable tension is a term in the finite difference equation so the tension could not be extracted from this equation,

the tension is required to calculate the displacements. However, knowing the displacements of the cable allows for the calculation of the strains of the cable segments between the nodes. Upon calculating the change in strains between time steps, the change in tension of the cable follow directly by summing the strains along the cable and utilizing basic mechanics which relates the strain to the tension [26]

$$\Delta T = \frac{\Delta L}{L_0} \times A \times E \tag{12}$$

where A is the cross-sectional area of the cable and E is the modulus of elasticity. As mentioned in Chapter 2, the modulus of elasticity for wire rope ranges from 10,000 and 14,000 ksi (68.95 and 96.53 GPa) [15]. This range in the value of E can influence the outcome of the computer model to a certain extent. For input to the computer model the mid-range value of 12,000 ksi (82.74 GPa) was used. The tension is used to calculate displacements at the next time step, after which a new tension is determined and so forth. This was the first approach taken in determining cable tensions; it failed for two reasons. First, utilizing the strain of each cable segment would include local strain created by antisymmetric (even) modes, but as discussed in Chapter 1 [7,8], the antisymmetric modes create no overall change in the tension of a cable. Second, the finite difference treatment of this problem

does not include the additional nonlinear aspect of longitudinal motion, the location of the nodes along the cable is fixed. When calculating strain of a segment based on a constant Δx, very large strains can occur when the slope of a cable segment is steep. Ideally, the Δx of the segment would decrease to compensate for the steep slope, but this was not allowed to happen with the consequence that very large strains occur. The combination of these two factors resulted in extreme overcalculations of the tension in the skyline with rapid instability of the model due to ever increasing tensions. A change in approach was called for.

The first symmetric mode is the mode primarily responsible for fluctuations in the tension of a cable. Based on this premise the strain in the portion of the skyline between the tailhold and point of excitation was determined using the Pythagorean theorem, with the distance from the tailspar to the excitation point and the displacement of the excitation point as input, and assuming that the distance between the tailhold and block on the tailspar remain constant (see Appendix F). The length of cable between the tailhold and block must be included because the skyline continues over the block and this length of cable contributes to the strain of the cable between the tailspar and point of excitation (this strain is accounted for in the Pythagorean calculation). Trial runs of the computer model utilizing this approach

yielded satisfactory results. Again, the tension was calculated at each time step based on the displacement of the excitation point at that same time step and then that tension was used as input to calculate the displacements along the cable for the next time step.

Damping

Damping was not included in the model. The inclusion of damping does not appear to be useful because the overall range of the skyline tensions during oscillation is the desired output, not necessarily the damped time history. The cable logging system used to verify the computer model had a damping of about three percent.

Incline of Skyline

Inclination of skylines, more correctly the chord of the skyline, depends on the terrain being logged and can range from horizontal to about 50 degrees (120 percent). To allow for incline of the skyline in the computer model would require a vector treatment of the cable displacements that was not included in this model. The use of this model should, therefore, be limited to skylines with small chord inclinations. The error that would be introduced in the transverse displacements of the skyline by using the program for a skyline with a slight chord inclination would be similar in magnitude to the error which occurs in approximating the cosine of a small angle as one.

The previous discussion has outlined the thought

process and decisions that went into the design of the program written to model the dynamic behavior of the skyline. The development of the computer model was accomplished in two steps:

1) Nonlinear model of a simple cable, considering transverse displacements only;
2) Nonlinear model of a cable with a large point mass (carriage and log load) capable of reproducing the hang-up/breakout phenomenon, again considering transverse displacements only.

Common procedures (the program is in Turbo Pascal) contained in both of the models are: Input, determination of initial conditions, solution for displacements, calculation of skyline tension and output.

Basic required input is:

- chord distance from tailspar to yarder;
- length of skyline from tailspar to tailhold;
- diameter of skyline;
- modulus of elasticity of skyline;
- initial tension in skyline;
- weight per foot of skyline;
- acceleration of gravity;
- spacing between nodes along skyline;
- size of time step;
- length of time history analysis;
- distance from tailspar to excitation point;

- amount of initial displacement at excitation point;

Output is a time history of the skyline tensions.

Modifications for the final model included additional inputs required, the weight of the carriage and estimated load the logs would place on the skyline plus the procedure for calculating the displacement of the point mass created by the carriage.

A flow diagram for the computer model is shown in Figure 15 and the program code for the final model is contained in Appendix G.

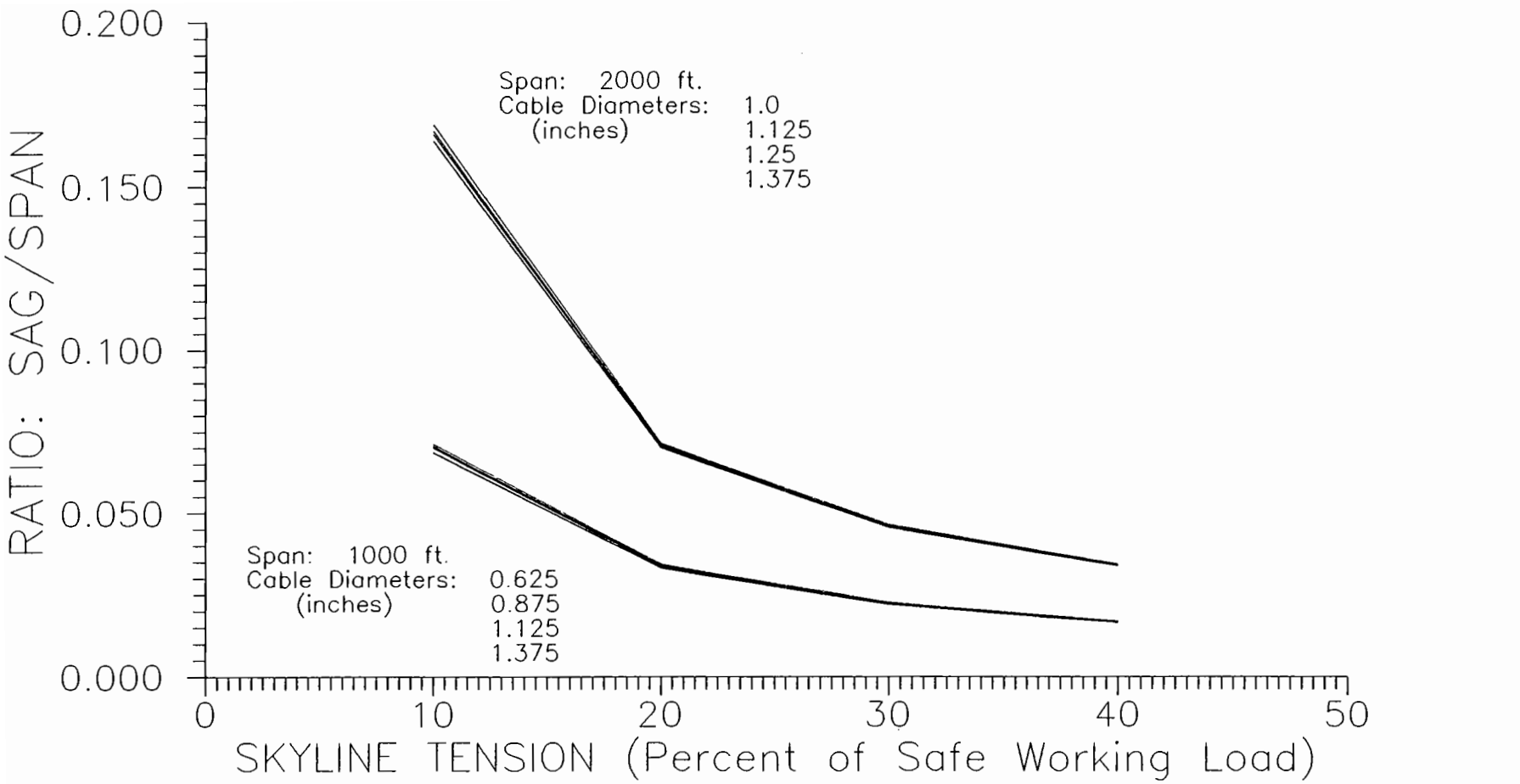

FIGURE 7 – SAG TO SPAN RATIO, SIMPLE CABLE

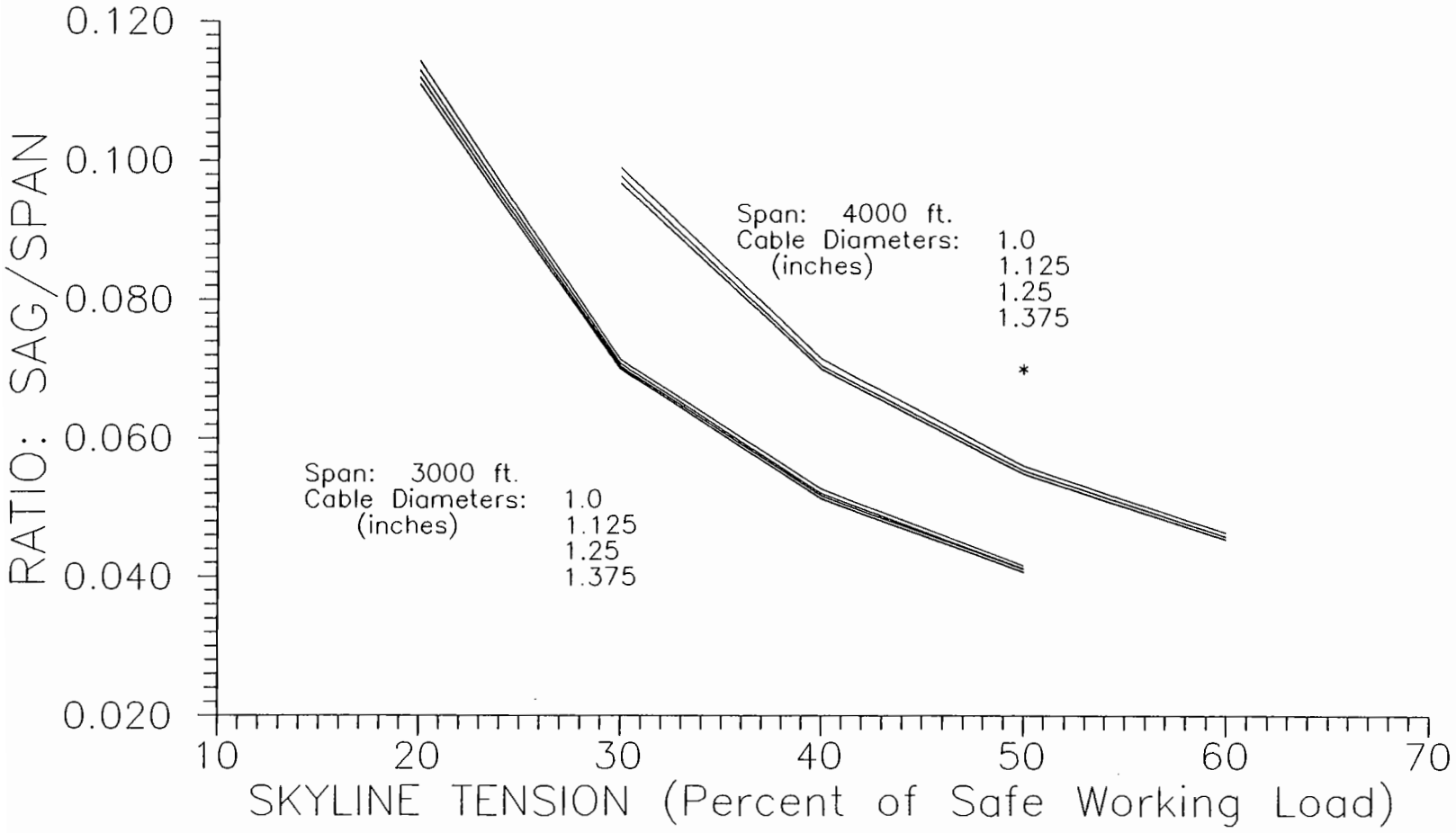

FIGURE 8 – SAG TO SPAN RATIO, SIMPLE CABLE

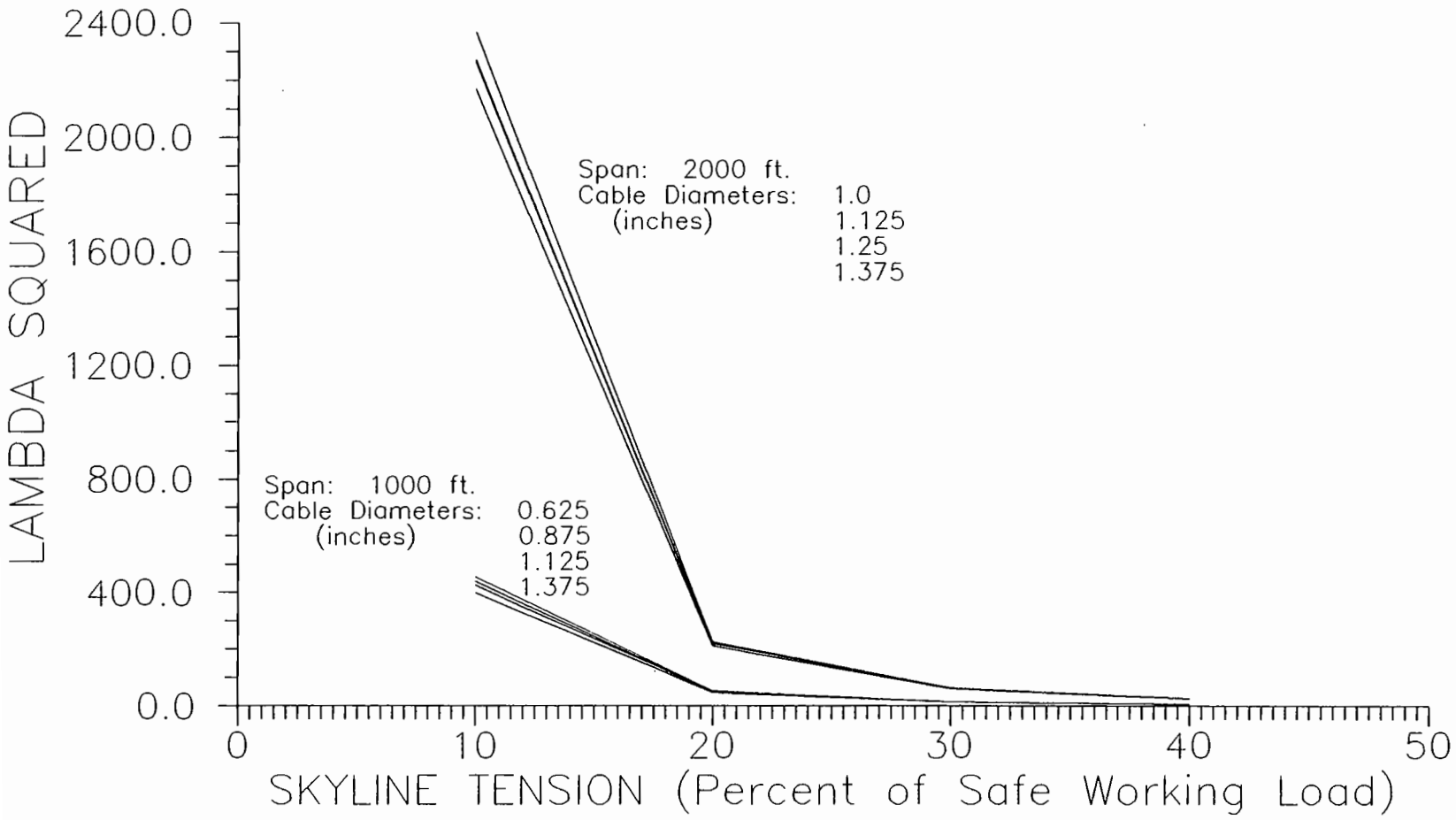

FIGURE 9 – LAMBDA SQUARED, SIMPLE CABLE

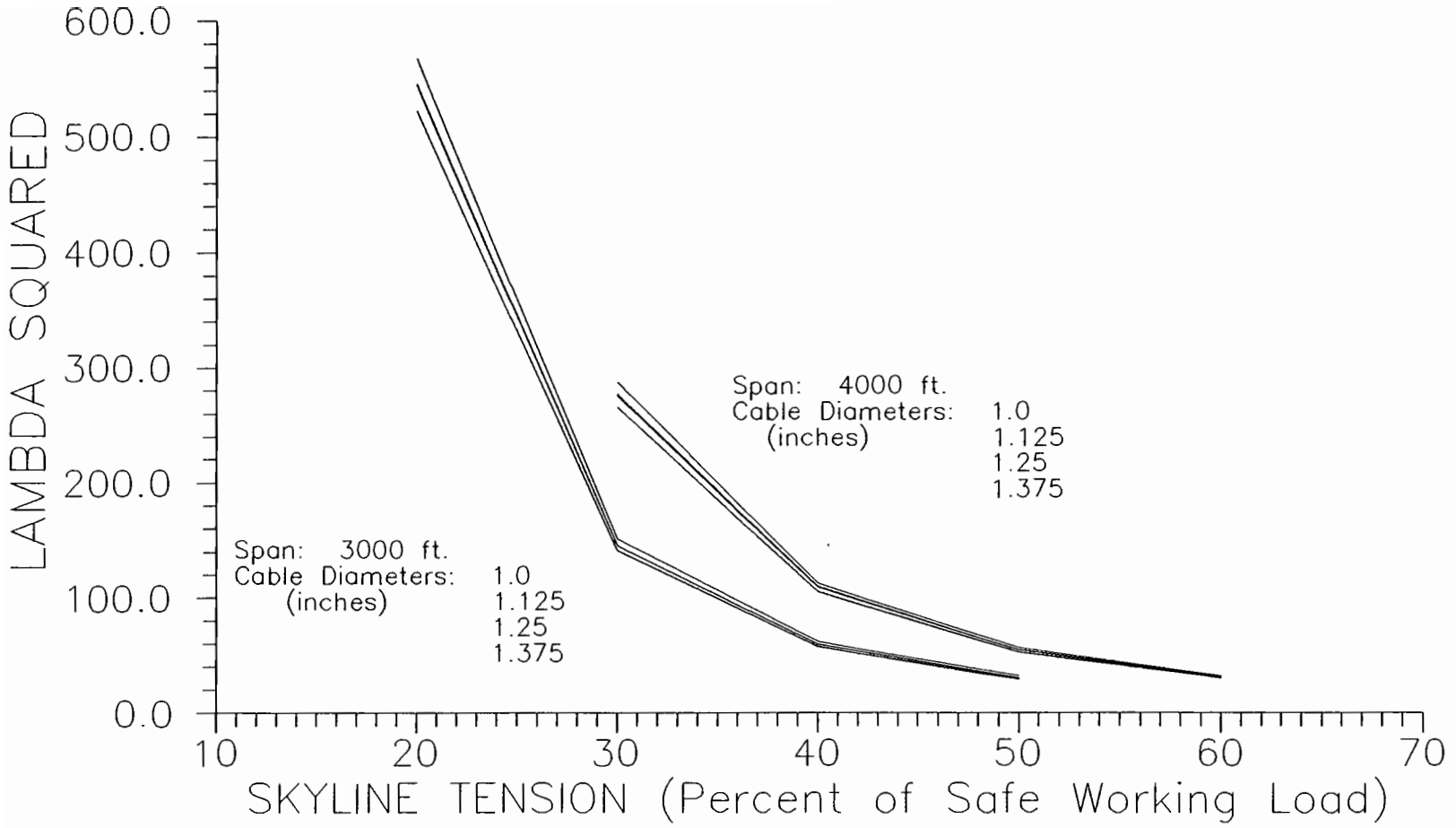

FIGURE 10 – LAMBDA SQUARED, SIMPLE CABLE

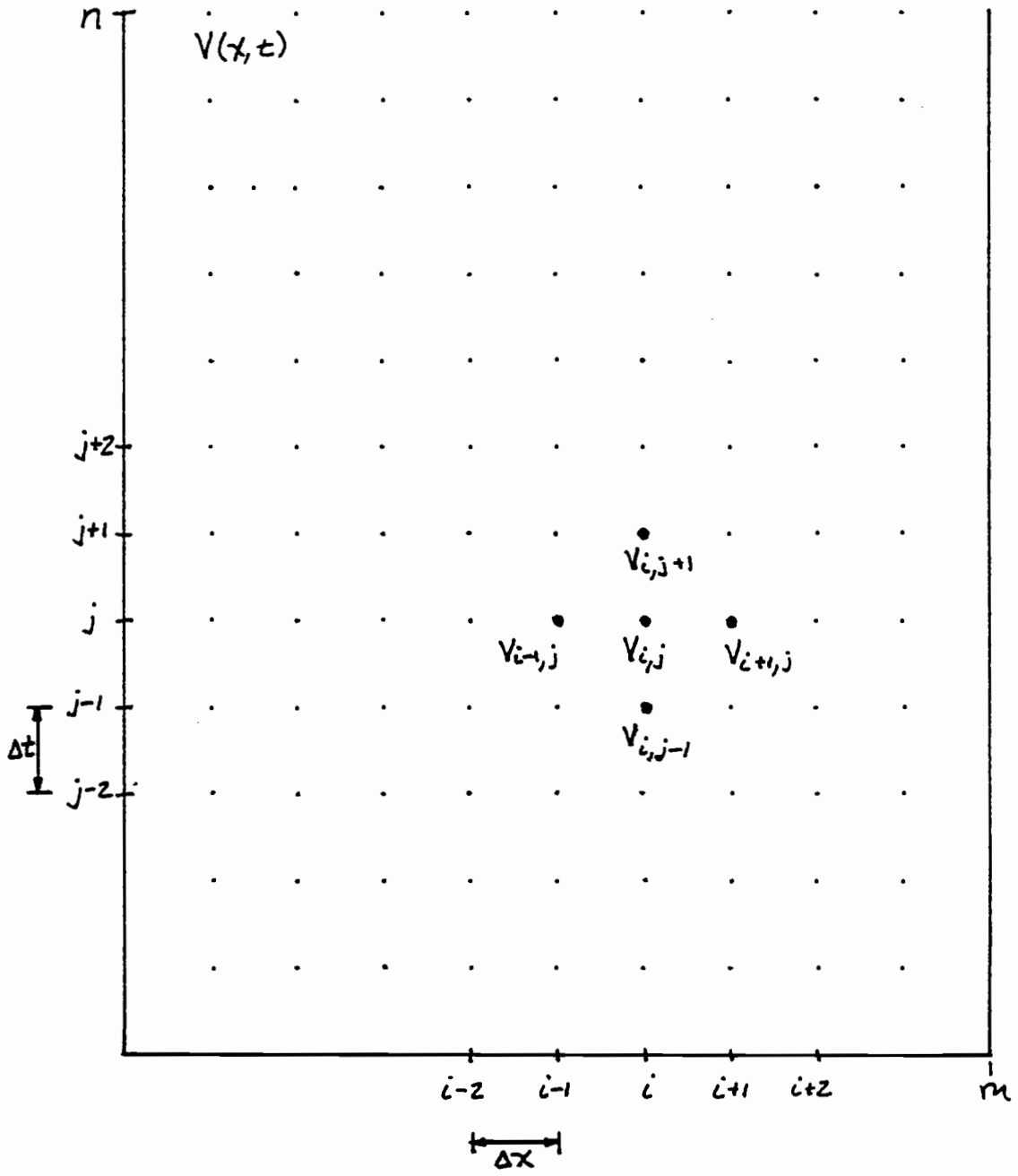

$$V_{i,j+1} = \frac{T(\Delta t)^2}{\rho(\Delta x)^2}\left(V_{i-1,j} - 2V_{i,j} + V_{i+1,j}\right)\left(\frac{\cos\theta}{\sqrt{1+\left(\frac{\partial V}{\partial x}\right)^2}}\right) + 2V_{i,j} - V_{i,j-1}$$

FIGURE 11
Five Point Finite Difference Scheme

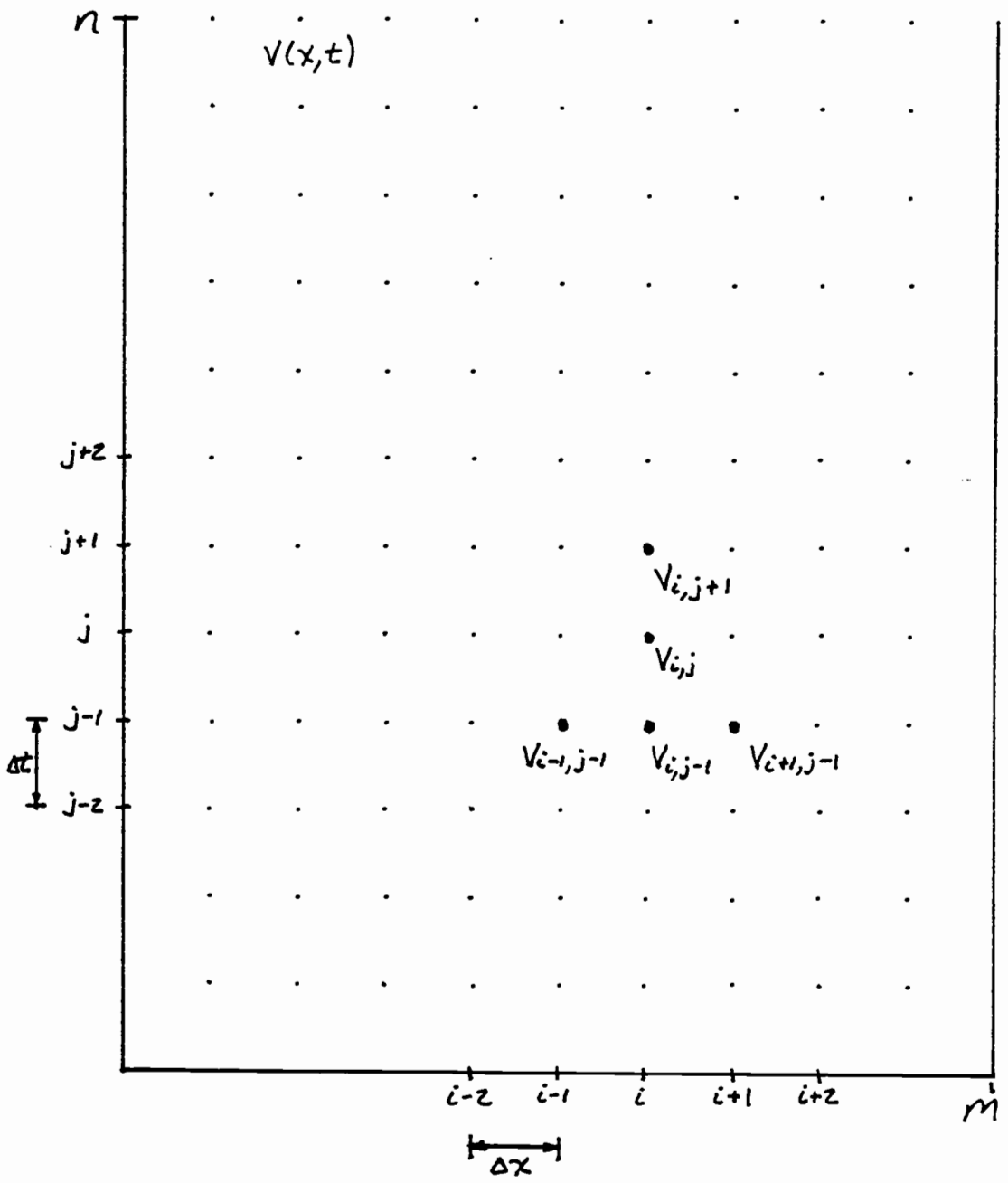

$$V_{i,j+1} = \frac{T(\Delta t)^2}{\rho(\Delta x)^2}\left(V_{i-1,j-1} - 2V_{i,j-1} + V_{i+1,j-1}\right)\left(\frac{\cos\theta}{\sqrt{1+\left(\frac{\partial V}{\partial x}\right)^2}}\right) + 2V_{i,j} - V_{i,j-1}$$

FIGURE 12 – Alternate #1
Five Point Finite Diffference Scheme

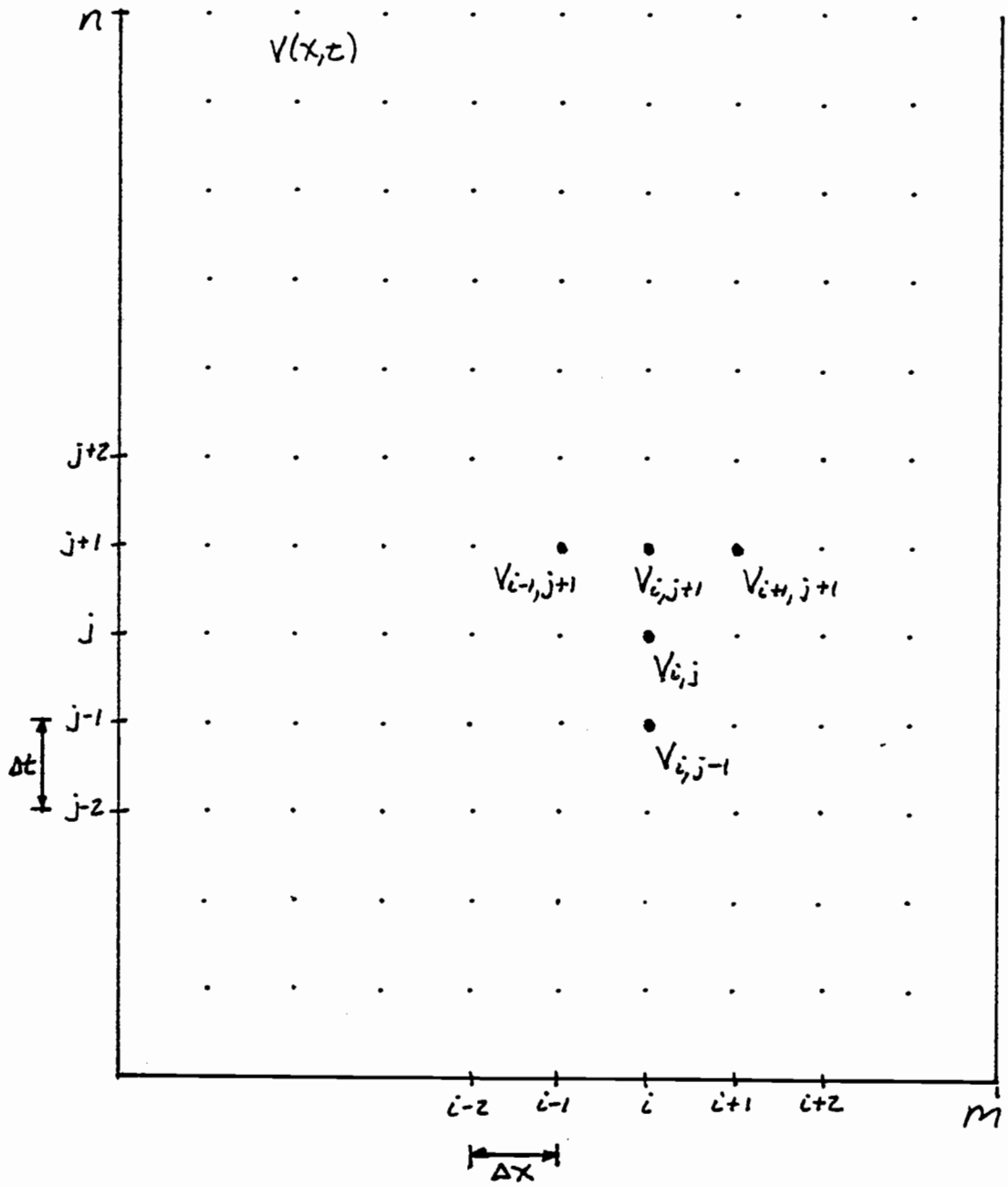

$$V_{i,j+1} - \frac{T(\Delta t)^2}{\rho(\Delta x)^2}\left(V_{i-1,j+1} - 2V_{i,j+1} + V_{i+1,j+1}\right)\left(\frac{\cos\theta}{\sqrt{1+\left(\frac{\partial V}{\partial x}\right)^2}}\right) = 2V_{i,j} - V_{i,j-1}$$

FIGURE 13 – Alternate #2
Five Point Finite Difference Scheme

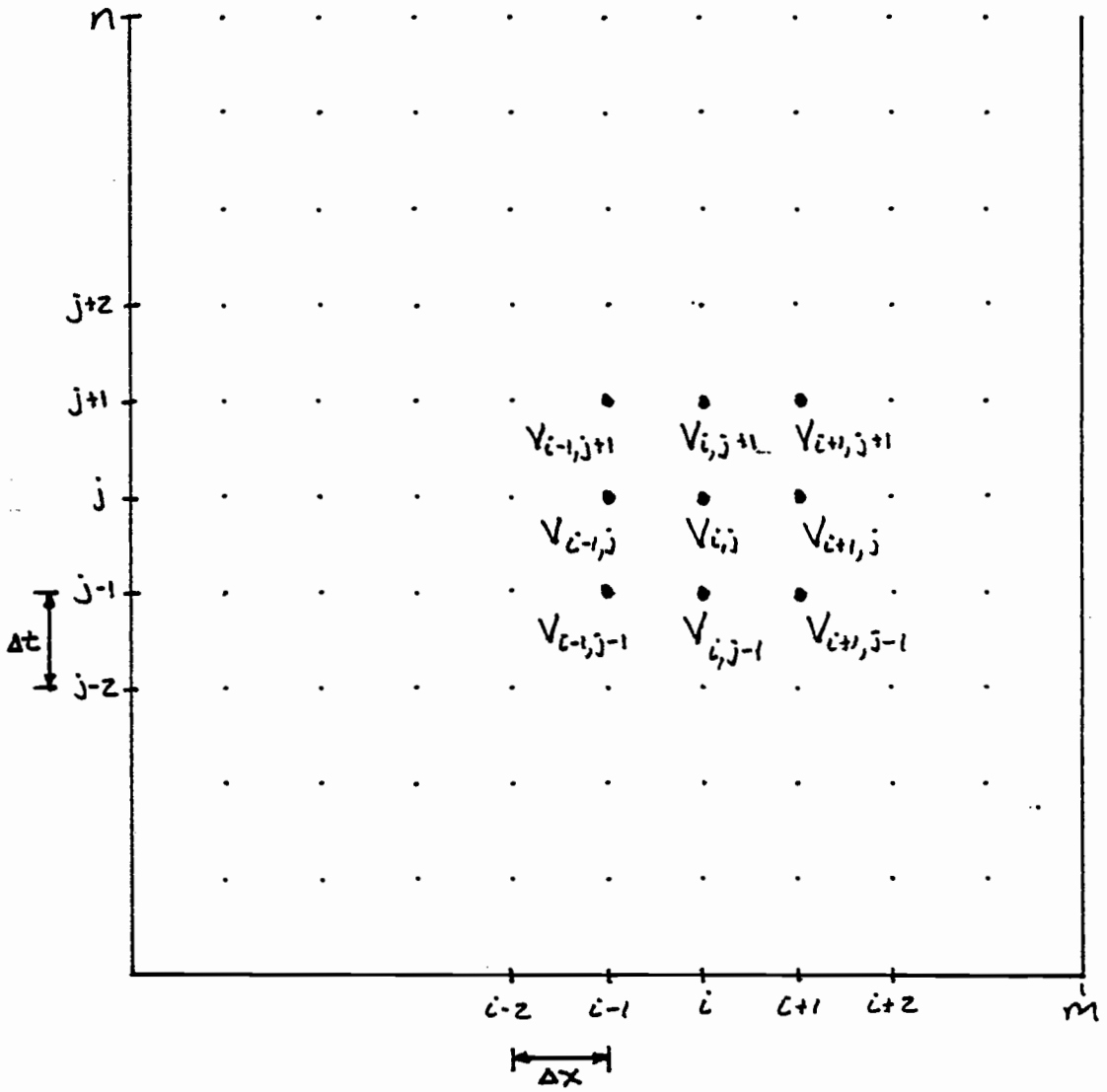

$$\delta^2_{\Delta x} V_{i,j} = V_{i-1,j} - 2V_{i,j} + V_{i+1,j} \qquad \delta^2_{\Delta t} V_{i,j} = V_{i,j-1} - 2V_{i,j} + V_{i,j+1}$$

$$\delta^2_{\Delta t} V_{i,j} = \frac{T(\Delta t)^2}{\rho(\Delta x)^2}\left(\frac{\delta^2_{\Delta x} V_{i,j-1} + 2\delta^2_{\Delta x} V_{i,j} + \delta^2_{\Delta x} V_{i,j+1}}{4}\right)\left(\frac{\cos\theta}{\sqrt{1+\left(\frac{\partial V}{\partial x}\right)^2}}\right)$$

FIGURE 14
Nine Point Finite Difference Scheme

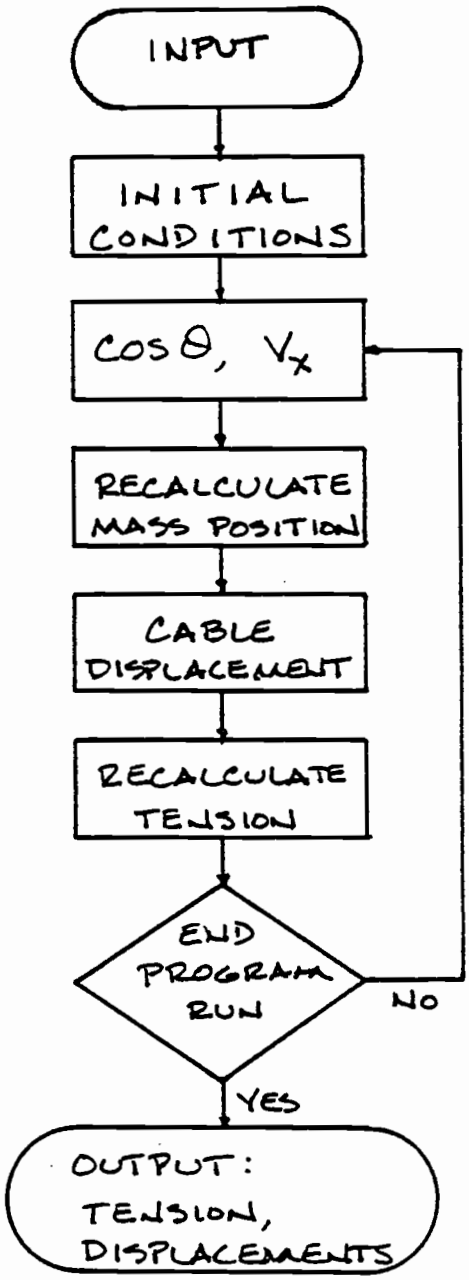

FIGURE 15 – FLOW DIAGRAM
FINITE DIFFERENCE PROGRAM

CHAPTER 6 - Experimentation

In order to check and verify the computer model a small cable logging system was erected in the McDonald Research Forest. The chord length of the skyline in this system was 330 feet (100 m) with a vertical rise of 25 feet (7.56 m), and an incline of 4.33 degrees or 7.58 percent. The diameter of the skyline cable was 5/8 inches (15.9 mm). Sag to span ratio for the simple cable with a tension of 4000 pounds (17.8 kN) was 1:127 and Λ^2 was 1.825.

The experimental setup, with the instrumentation, is shown in Figure 16. The accelerometers, placed at the half-point and quarter-point of the skyline, are small commercial quartz crystal devices which measure the accelerations of the object they are attached to, output is voltage which can be converted to g's. The load cells, fabricated by research assistants in the Forest Engineering Department, were placed in the skyline, dropline (choker) and on the strap which attaches the skyline block to the tailspar. They are metal bars with four strain gages, wired as a Wheatstone bridge, attached to them. When inserted at the end of a cable these load cells indicate the tension in the cable by outputting a voltage which is converted to pounds of load. The displacement transducers placed on the tail spar are commercially available devices which have a small wire wrapped around a spring loaded pulley connected to a five

or ten turn precision potentiometer contained within a housing. As the wire is pulled and released the pulley moves which creates a change in the resistance of the potentiometer. This change in resistance is reflected in a varying voltage output which is translated to displacement. An IBM XT computer was used to acquire and store the field data with the assistance of a commercial data acquisition software [19].

To determine the displacements of the skyline investigators originally intended to take the acceleration output of the accelerometers and perform double integration of these values knowing the appropriate initial conditions. Theoretically, this would have resulted in the dynamic displacements of the skyline; however, practically this was not the case. The output of the accelerometers was integrated twice using the trapezoidal rule on a spreadsheet. The results were simply mild oscillations of the skyline about its initial position. There was no evidence of the types of deflections that were actually occurring. There seemed to be a lack of sensitivity in the accelerometers in that they were not indicating the types of accelerations that must have been occurring in the skyline. After considering the possible reasons for the poor results, the most plausible explanation is as follows: the accelerometers are intended to measure the acceleration that occurs along their longitudinal axis, in the case of

the skyline this axis would be transverse to the chord of the skyline and in the plane of the system. A skyline under dynamic loading tends to rotate about two axes. First, the wire rope as it undergoes changes in tension twists about its own longitudinal, x, axis. Second, as the wave passes through the skyline this creates a rotation about the z axis which is transverse to the skyline and normal to the plane of the system (see Figure 17). Both of these rotations take the accelerometer out of its desired position and severely limits its sensitivity to the proper accelerations.

Though inconvenient, this problem was not fatal. The load cells functioned quite well throughout the experiments and since the most critical output of the computer model is the change in tension of the skyline it was decided to use this as the way in which the model could be verified. If computer model tensions compared favorably to field data of the skyline tensions, this would indicate a correct model which would necessarily require the displacements of the model to be similar to the displacements which were occurring in the field.

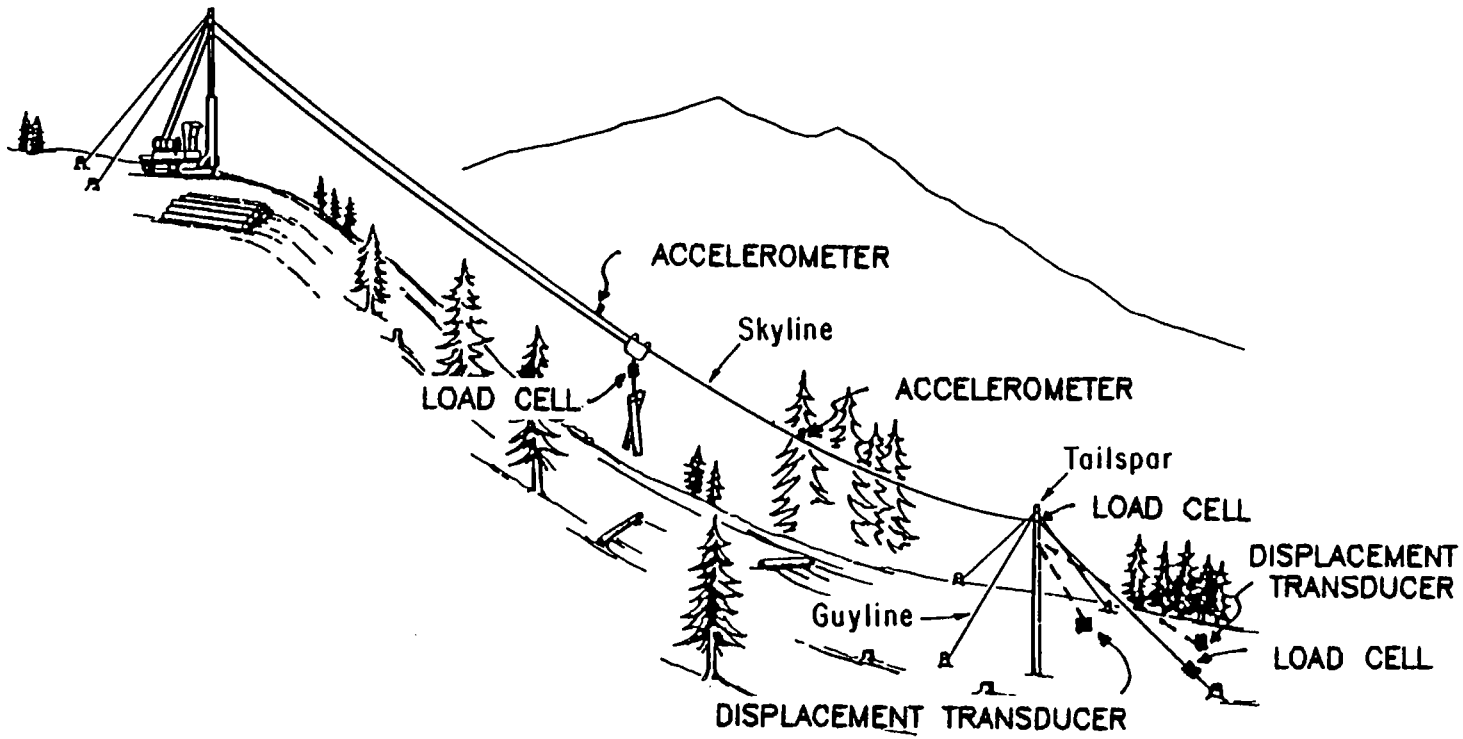

FIGURE 16 – Cable Logging System Instrumentation

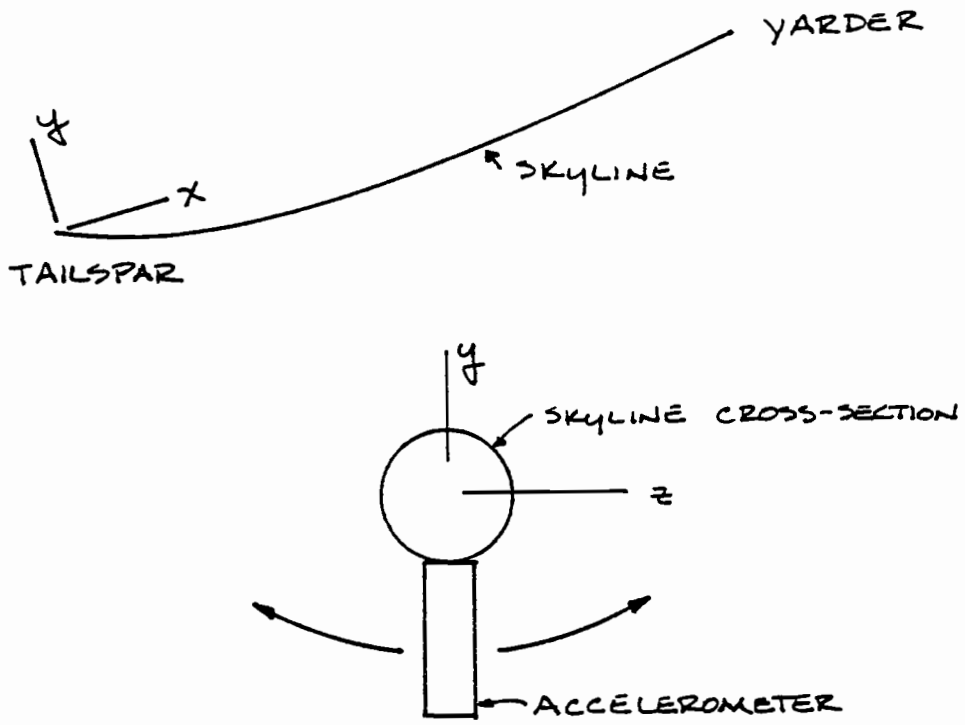

FIGURE 17 – Skyline Rotations

CHAPTER 7 - Verification of Preliminary Model

A preliminary model of a simple cable was conducted on the skyline described in Chapter 6 with no carriage or turn of logs (point mass). The skyline was tensioned from 4,000 lbs. to 10,000 lbs. (17.8 kN to 44.5 kN), which can be considered typical working tensions in a system of this configuration, in increments of approximately 2,000 lbs. (8.9 kN). At each load the skyline was "plucked"; pulled down a measured distance and released. The ensuing dynamic behavior was recorded. The "pluck" point, or point of excitation, for this series of tests was 112 feet (33.9 m) from the tailspar. The results of this series of four tests, in the form of skyline tension time histories, are shown in Figures 18 through 21.

Comparisons of model results to the field tests, and to linear theory in the case of frequencies, are shown in Figures 22 and 23 and tabulated in Table 1. The maximum error of the model compared to field data for frequencies is -12.0 percent at 4,000 pounds (17.8 kN) of skyline tension. The percent error of the model improves as the tension of the skyline increases.

With regard to the changes in the skyline tension as the skyline oscillates two values are compared: the maximum tension which occurs and the range of tensions, maximum to minimum, that results due to the skyline oscillations. The maximum error for maximum tensions predicted by the computer model is +4.48 percent at a

skyline tension of 4,000 pounds (17.8 kN) and, like the error of the predicted frequencies, improves as the tension in the skyline increases. The maximum error for the range of tension given by the computer model is 21 percent, at a skyline tension of 10,000 pounds (44.5 kN) and a minimum of two percent at a skyline tension of 8,000 pounds (35.6 kN).

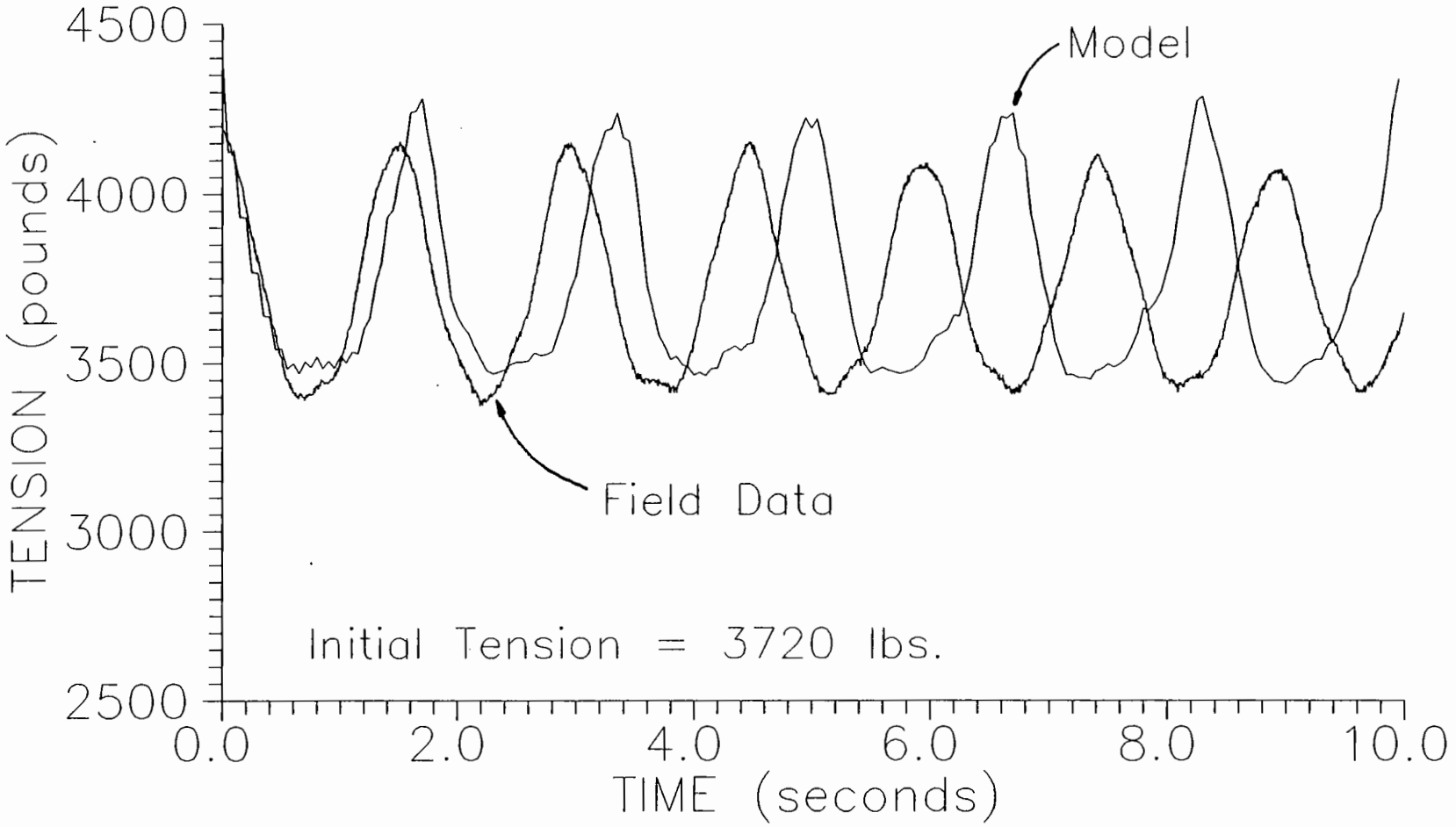

FIGURE 18 – SKYLINE TENSION, SIMPLE CABLE

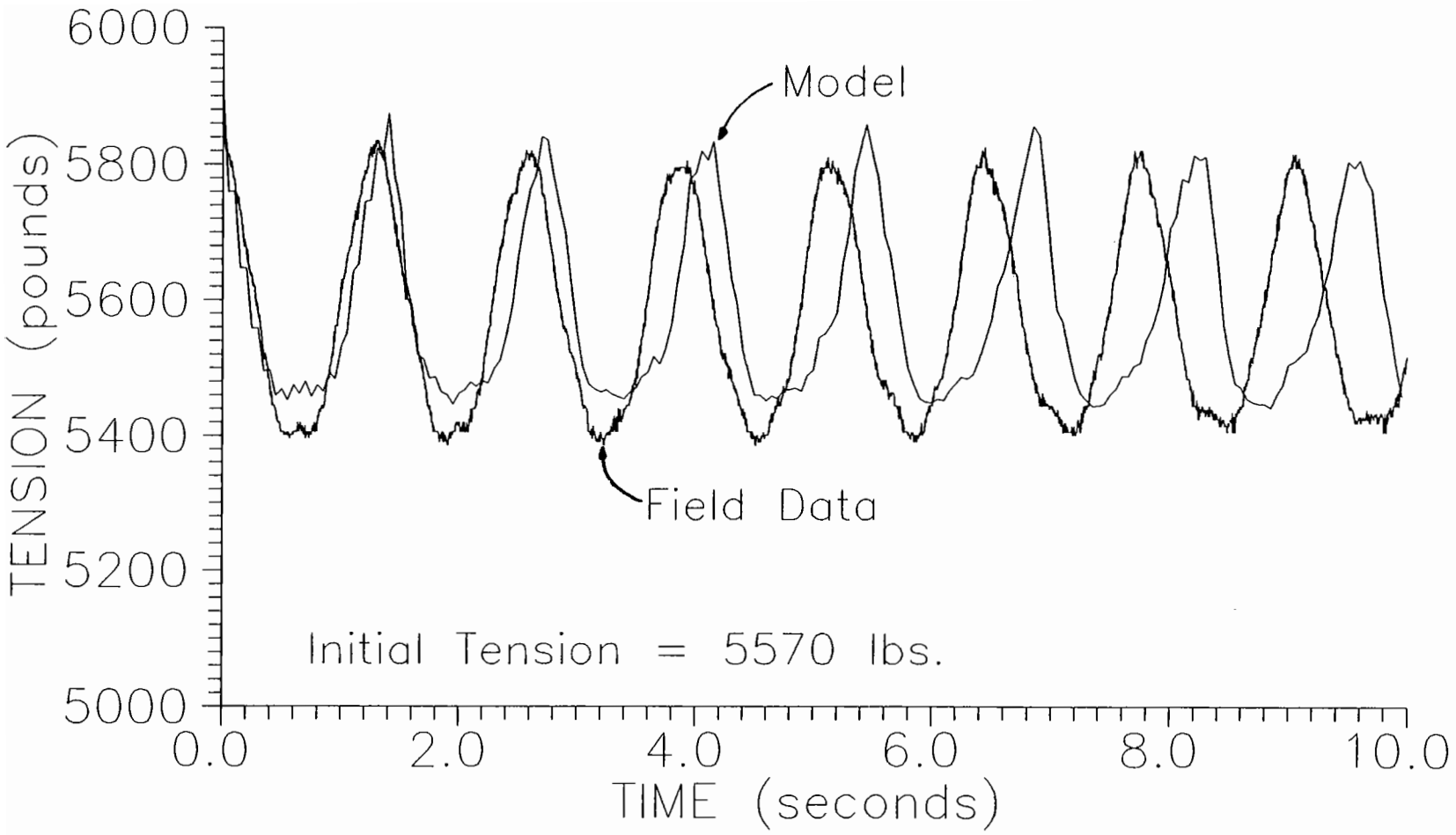

FIGURE 19 – SKYLINE TENSION, SIMPLE CABLE

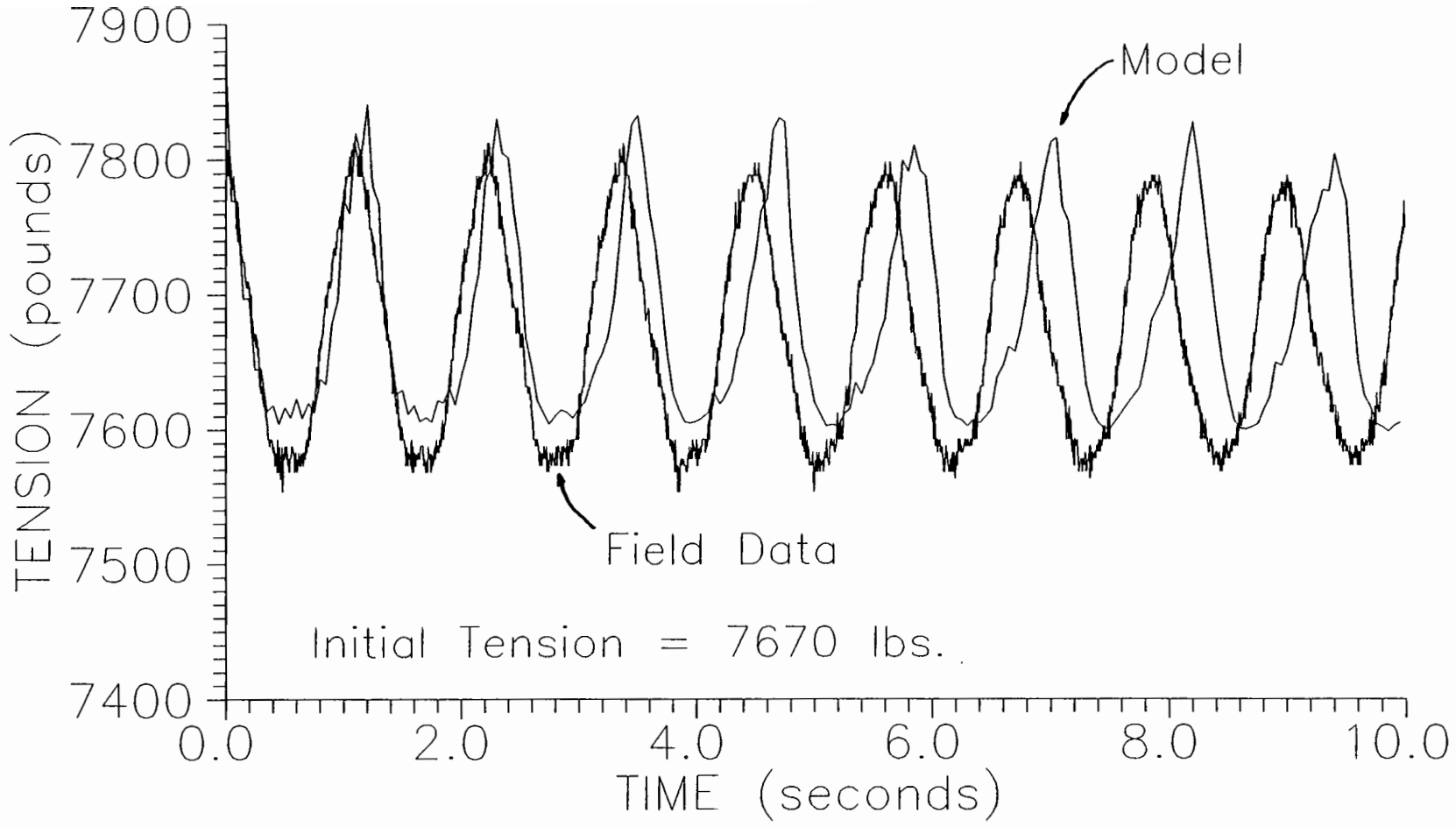

FIGURE 20 – SKYLINE TENSION, SIMPLE CABLE

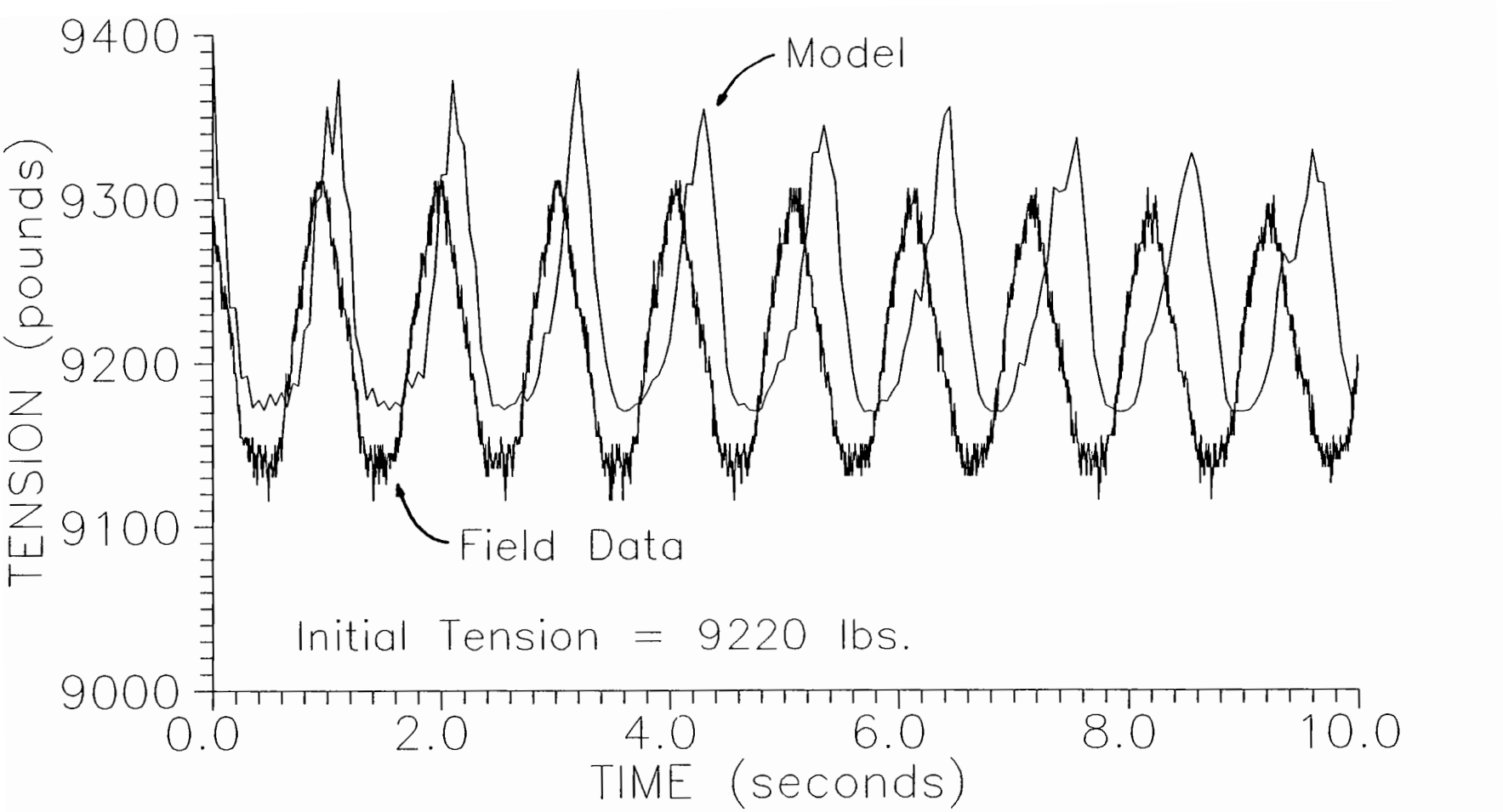

FIGURE 21 – SKYLINE TENSION, SIMPLE CABLE

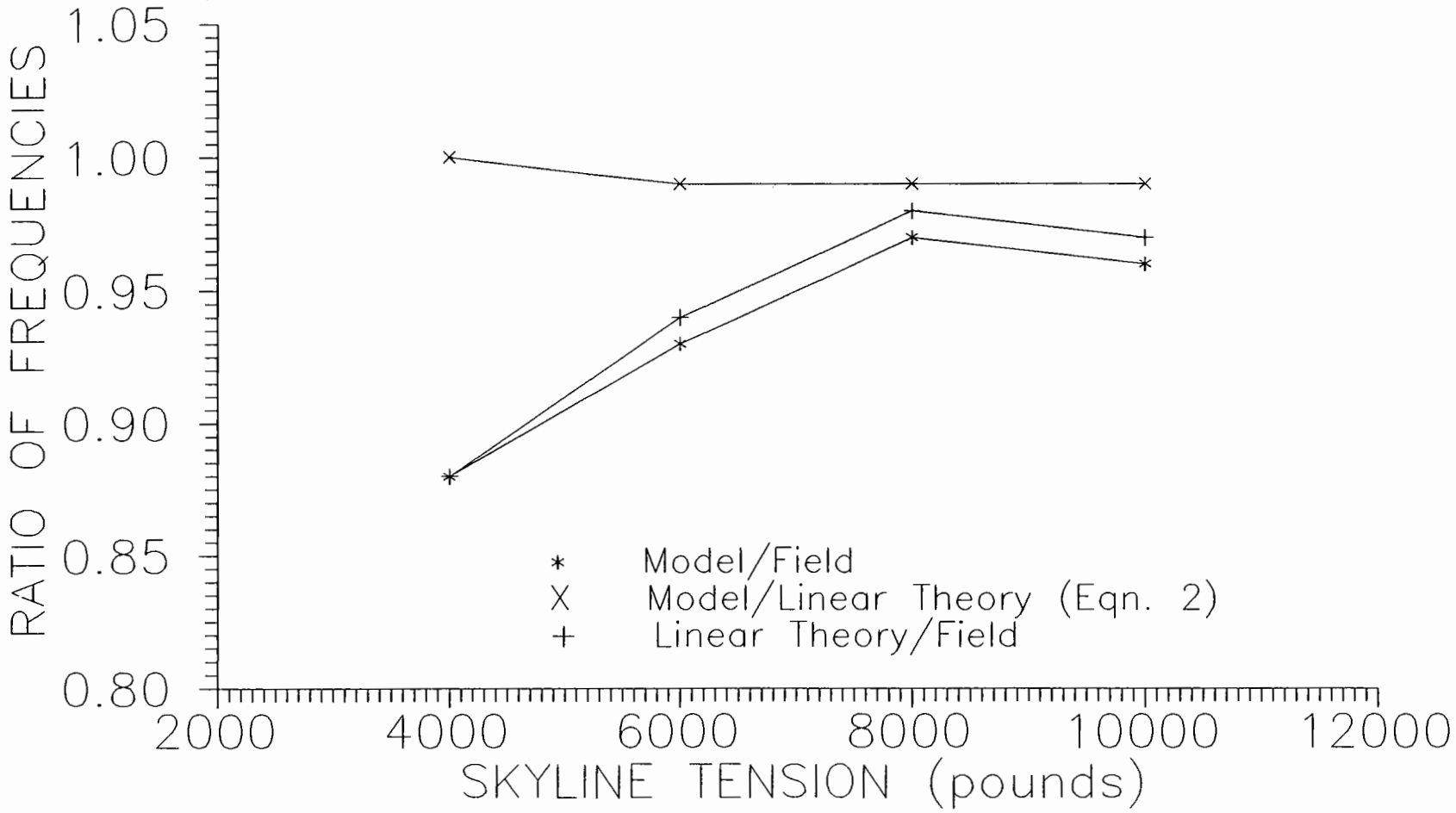

FIGURE 22 – COMPARISON OF MODEL TO FIELD DATA

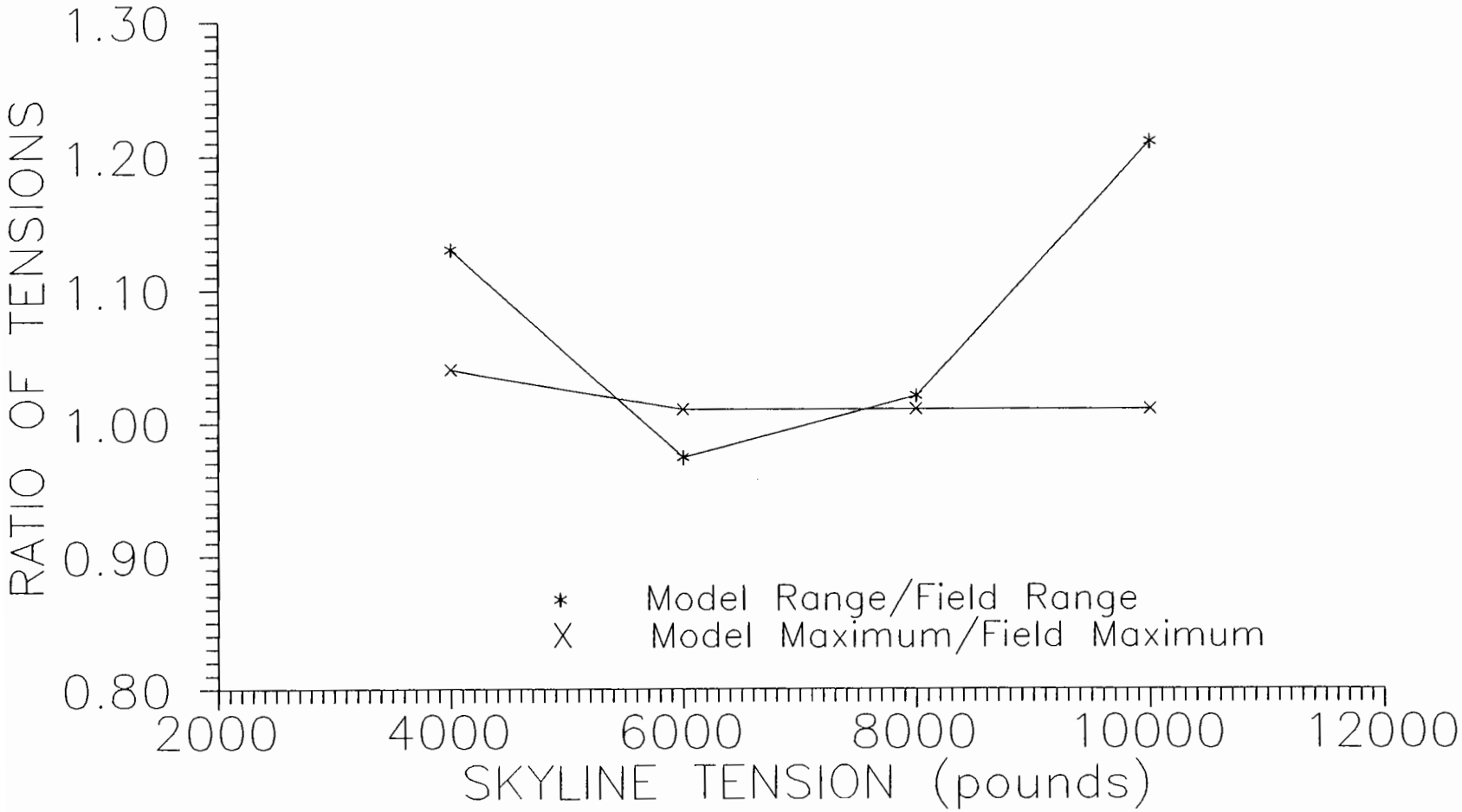

FIGURE 23 – COMPARISON OF MODEL TO FIELD DATA

TABLE 1 - Skyline Tensions

Comparison of Field Data and Computer Model

Equil. Tension	Maximum Tension* Field	Model	% Error Model	Minimum Tension* Field	Model	% Error Model	Frequency (Hz) Field	Model	Theory Eqn. 2
3720	4194	4382	4.48	3383	3468	2.51	0.684	0.602	0.600
5570	5849	5909	1.03	5385	5457	1.34	0.781	0.729	0.735
7670	7812	7868	0.72	7553	7604	0.68	0.879	0.851	0.862
9220	9301	9395	1.01	9116	9171	0.60	0.977	0.938	0.945

* Tension measured in pounds.

CHAPTER 8 - Verification of Final Computer Model

The final version of the computer model attempted to duplicate the dynamic behavior of the skyline as the turn of logs hang-up and break out while the yarder continues to pull in the carriage. In the field this event was simulated by bringing the skyline up to the desired tension, tying the log load to a stump with a nylon rope and then engaging the yarder to reel in the carriage/log load until the rope broke. These tests were conducted at sporadic distances along the skyline because of the location of useable stumps to tie the rope to. This method worked fairly well, of seven tests run, five produced useable data for comparison with the computer model. Data collected from the field tests for the behavior of the skyline is overlaid on output from the computer model, in the form of skyline tension time histories, in Figures 24 to 28. For these computer simulations a distance of 0.5 feet (0.15 m) was used between nodes and 0.05 seconds was the size of the time step. A ten second simulation would take 20 minutes to run on an AT clone with an 80286 processor and an 80287 math coprocessor, running at over 12 MHz. A summary of model and field data is contained in Table 2.

Analysis

The maximum error for the computer model with respect to the skyline frequencies occurred in the first field test where the error was 16.2 percent. The computer model

did quite well in predicting the frequencies of the other four field tests with the magnitude of errors being 6.41 percent or less, see Figure 29.

The error in computer model calculations of maximum skyline tensions were within ±5.16 percent for all tests, see Figure 30. The range of tensions seen as the skyline oscillates were a little more erratic. The maximum error was -20.1 percent for the last field test, with the error improving for the other tests to a magnitude of 11.3 percent or less.

The principal cause for the error in the computer model of the dynamic skyline behavior comes from the inability to determine exactly the conditions in the skyline logging system as the turn of logs breaks out after being hung-up. Part of the input necessary to start running the computer program is the displacement which occurs in the skyline due to the hang-up just as the logs break loose. In the field tests there was no way to physically measure this displacement, it was too dangerous to be near the turn of logs. Therefore, this displacement was determined from the recordings of the tensions in the skyline and dropline. Due to the lack of control in the field experiments (it is not easy to control a diesel yarder, 330 feet (100 m) of skyline and 1,000 pound (4.45 kN) log, where there was a lot of slippage, jerking, bouncing, etc. just prior to and following the breakout) some error was introduced when calculating the

displacement of the skyline as the turn of logs break loose. This error was then introduced to the computer model as part of the input to start the program, resulting in some disparities between model output and field test results.

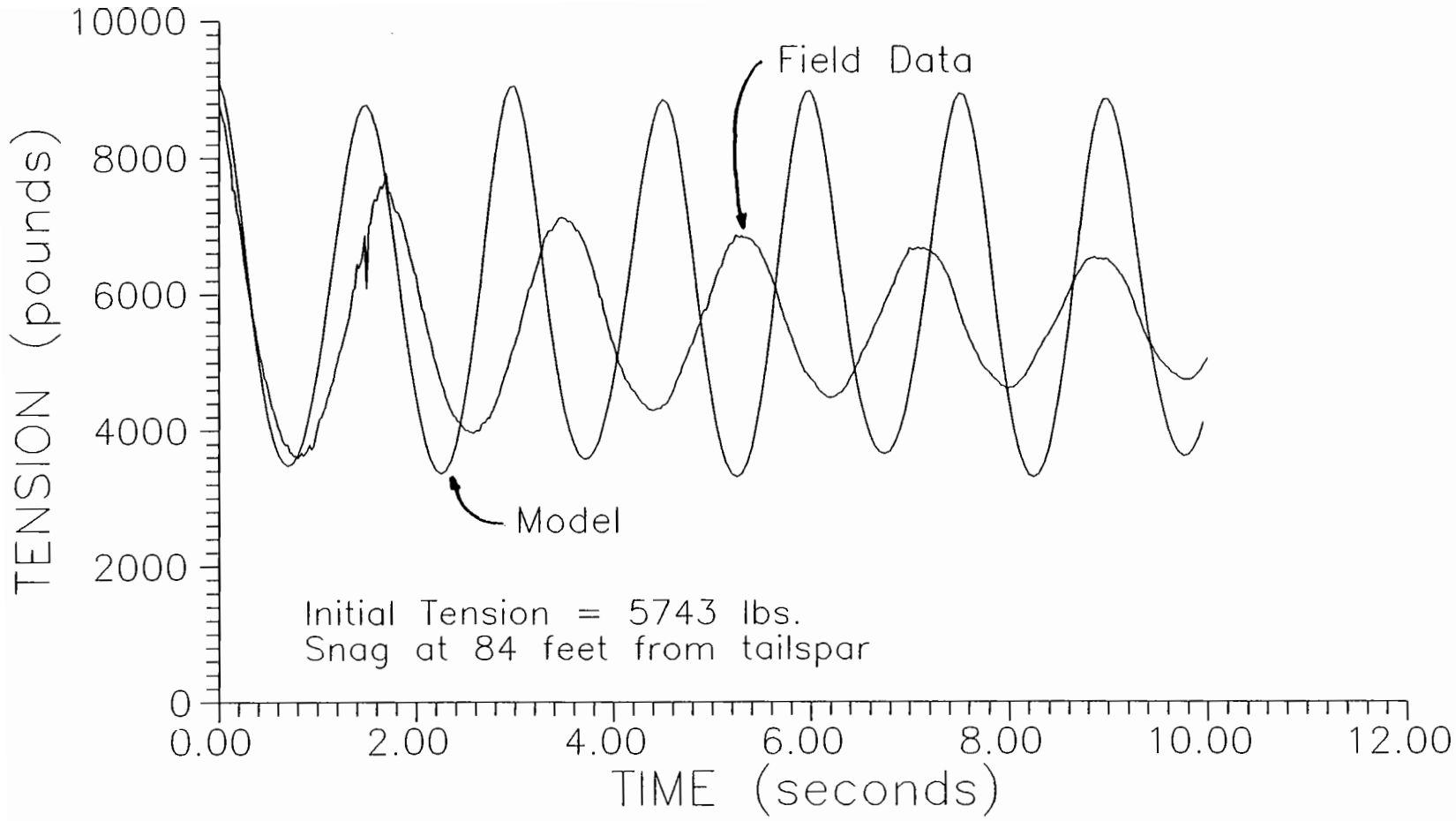

FIGURE 24 – SKYLINE TENSION, HANG–UP TEST #1

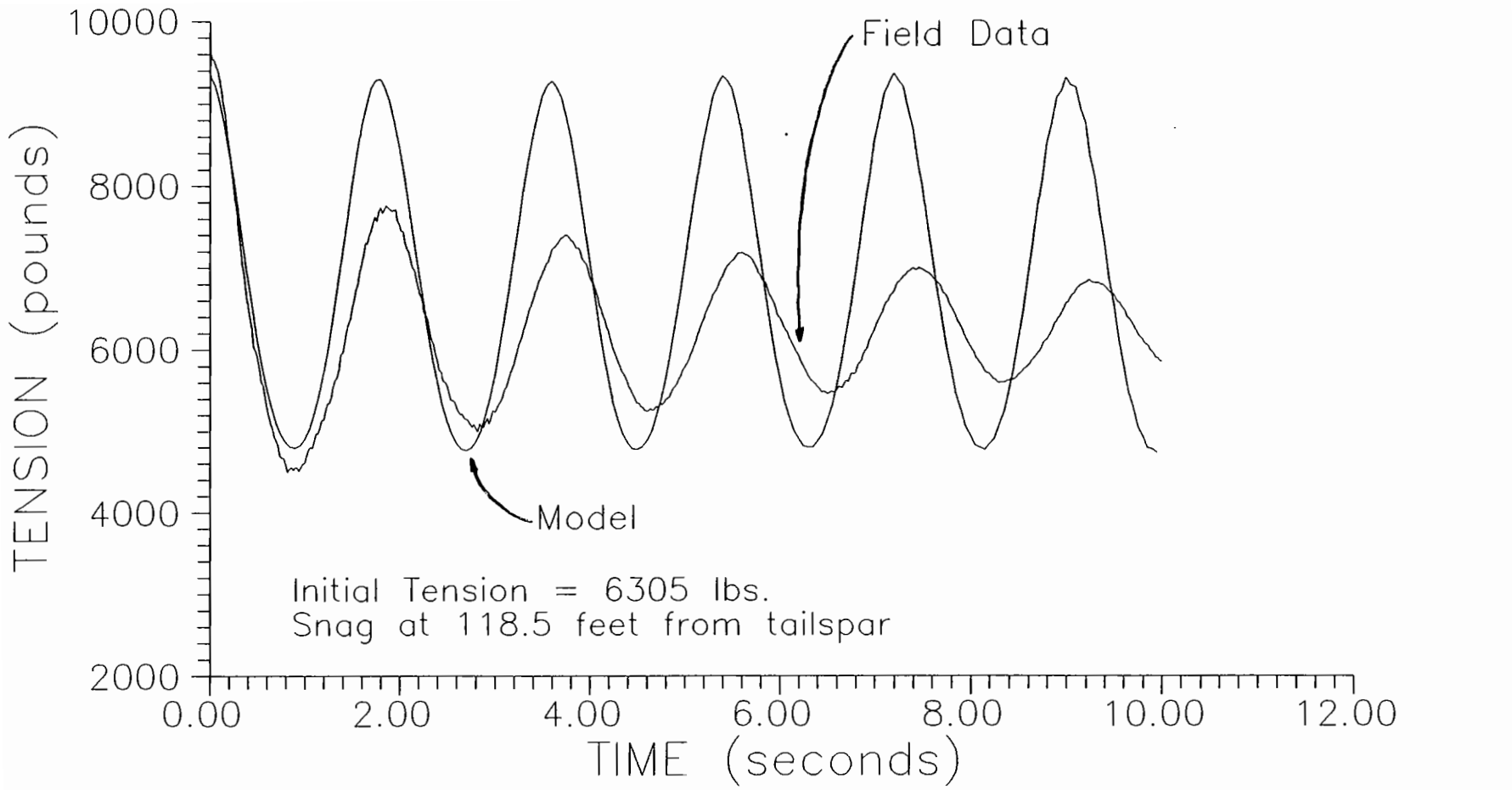

FIGURE 25 – SKYLINE TENSION, HANG–UP TEST #2

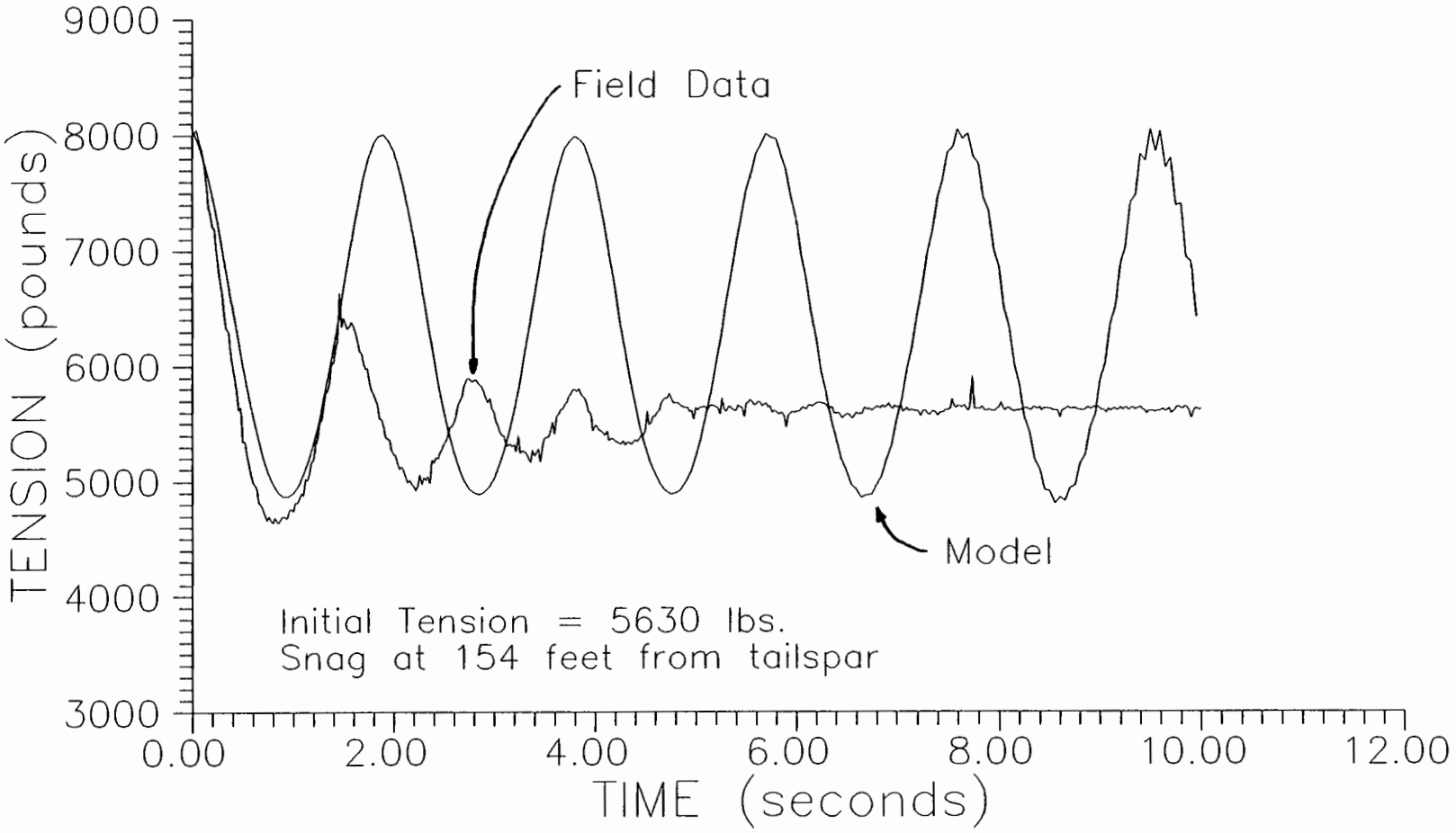

FIGURE 26 – SKYLINE TENSION, HANG–UP TEST #3

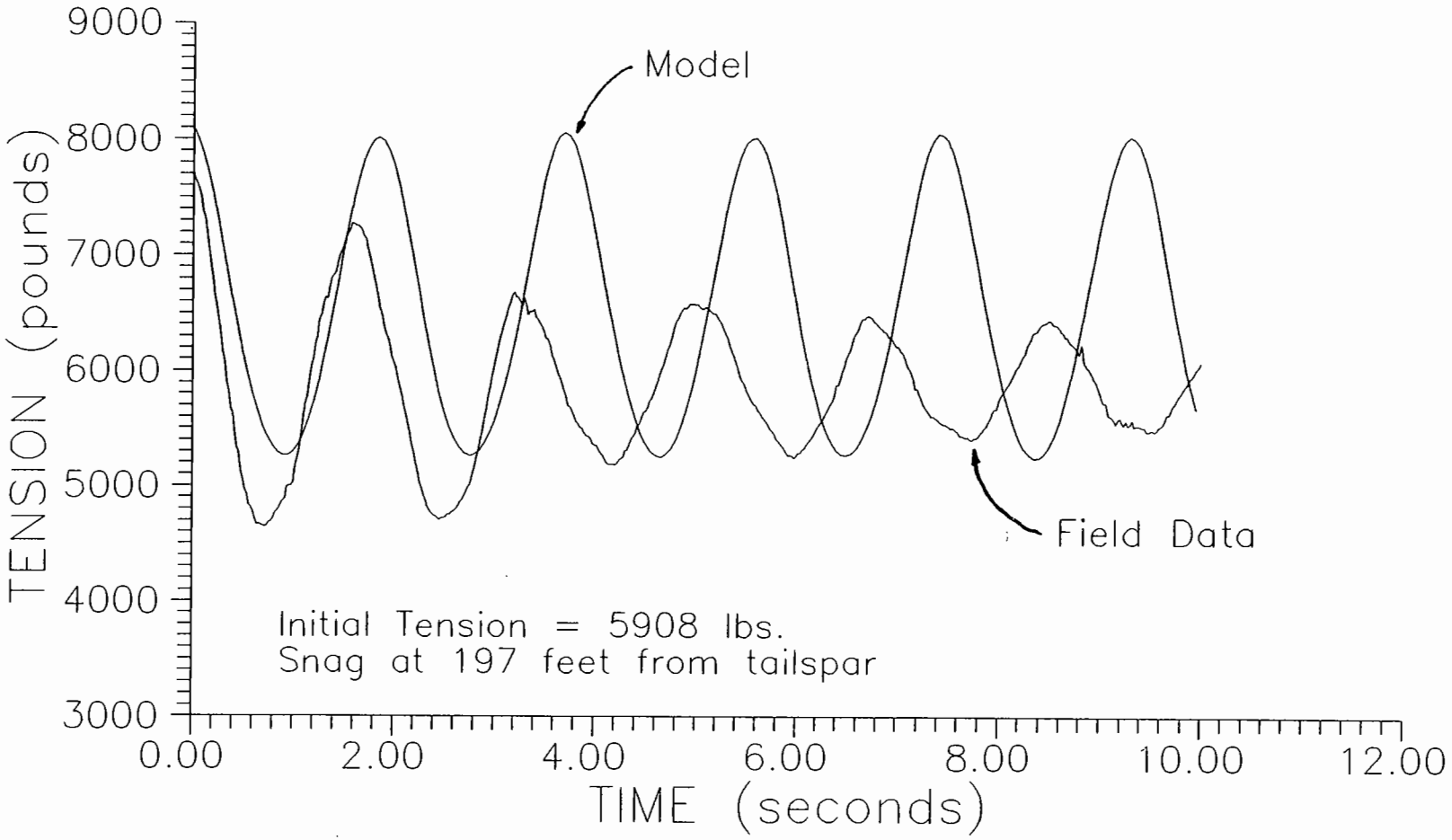

FIGURE 27 – SKYLINE TENSION, HANG–UP TEST #4

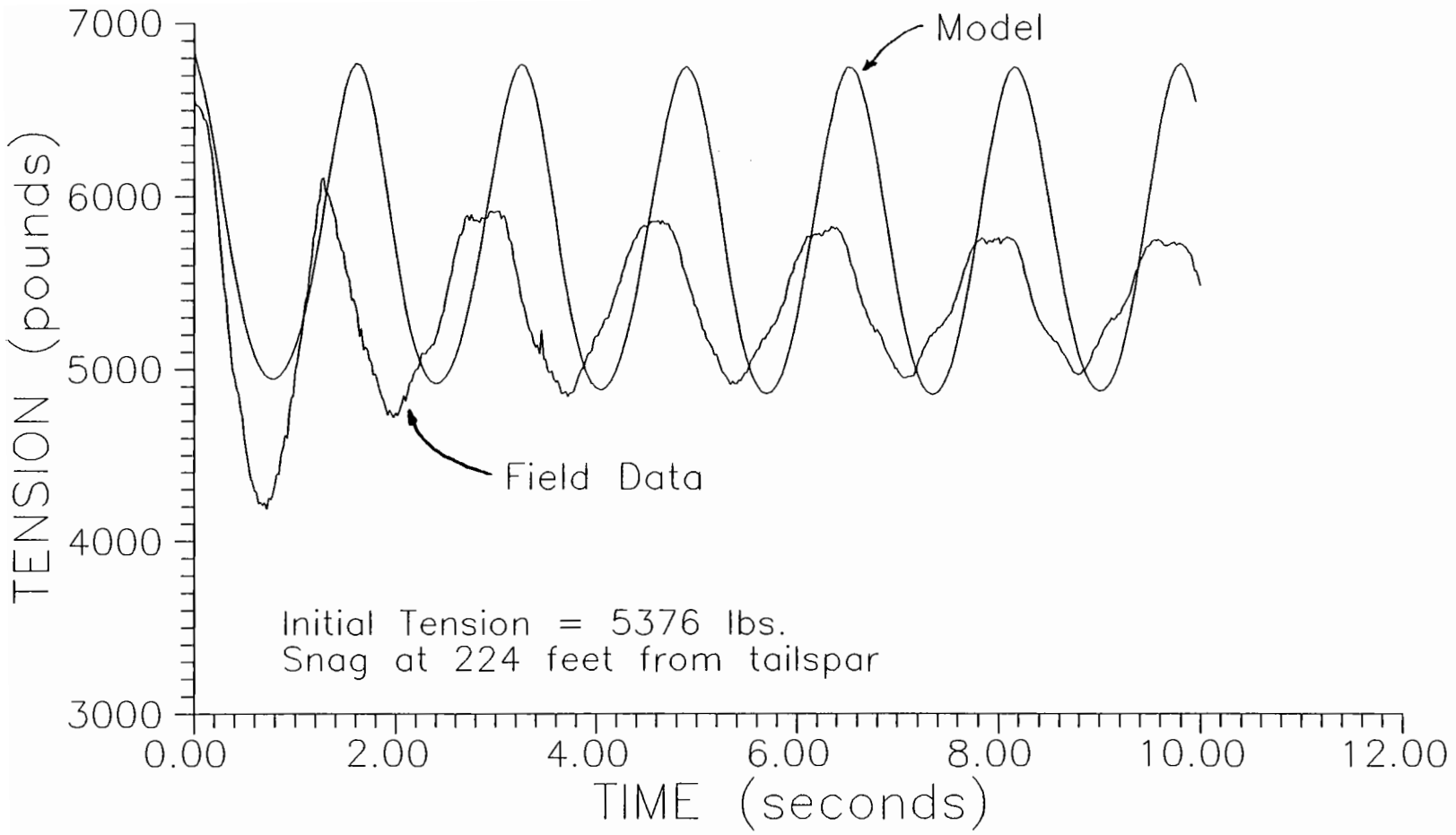

FIGURE 28 – SKYLINE TENSION, HANG–UP TEST #5

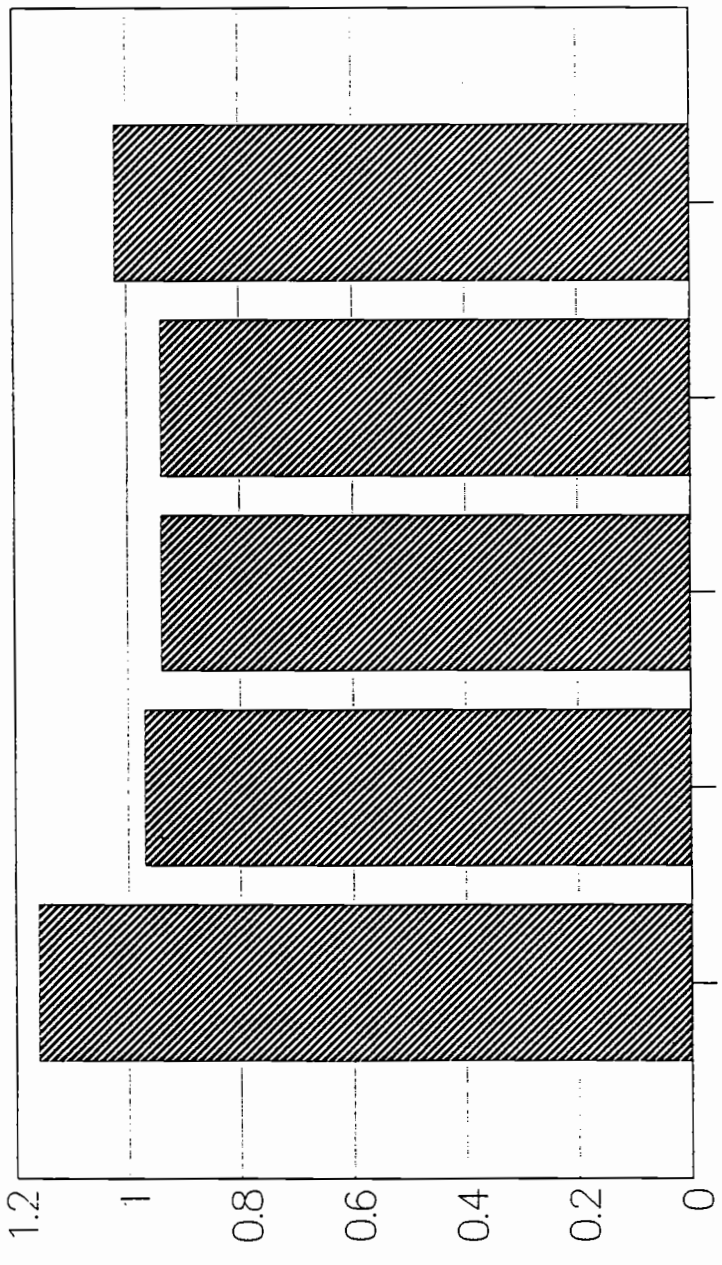

FIGURE 29 – COMPARISON OF MODEL TO FIELD DATA

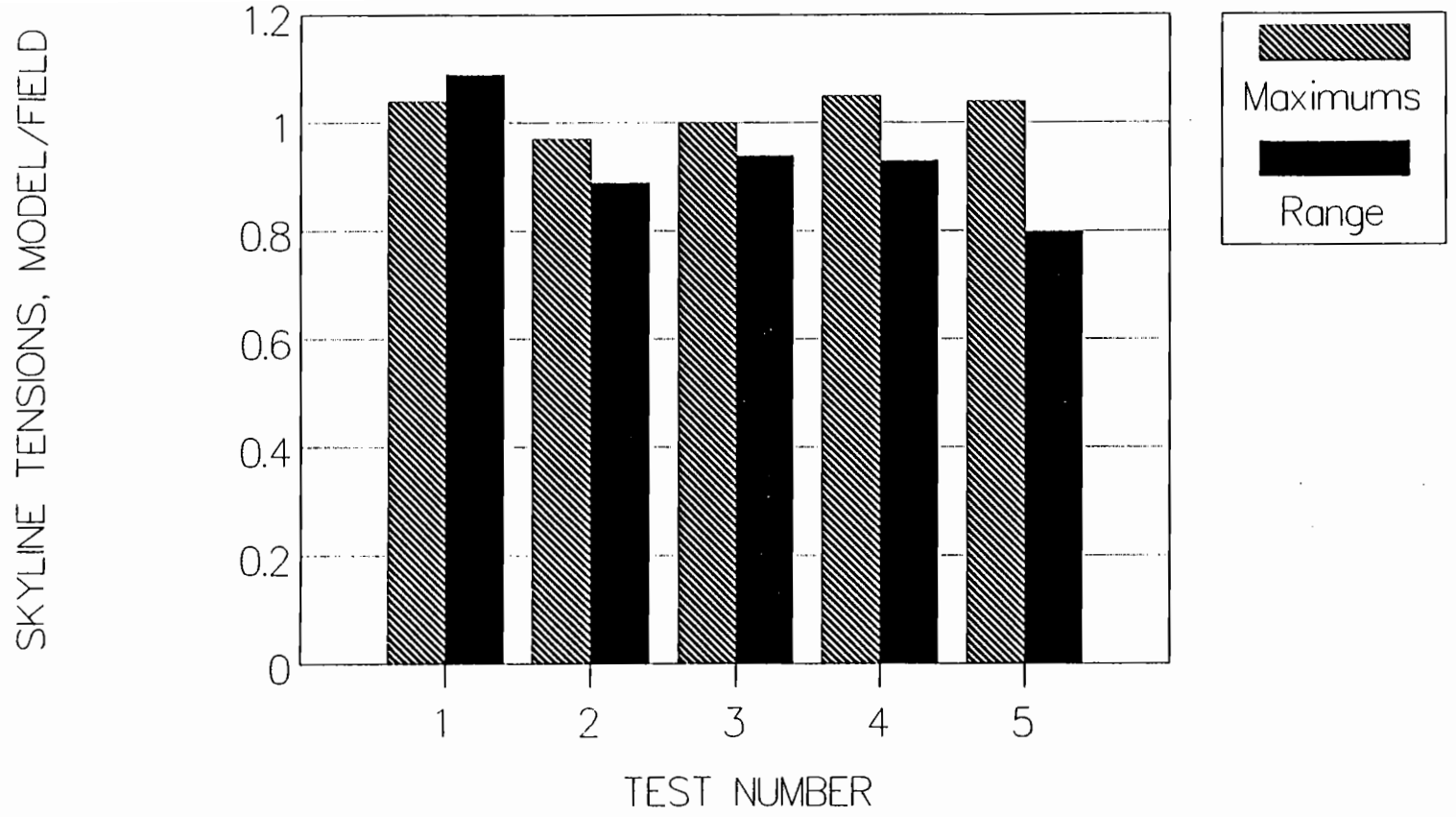

FIGURE 30 – COMPARISON OF MODEL TO FIELD DATA

TABLE 2 - Skyline Tensions

Comparison of Field Data and Computer Model

Test No.	Log Load From TailSpar	Equil. Tension	Maximum Tension*			Minimum Tension*			Frequency (Hz)		
			Field	Model	% Error Model	Field	Model	% Error Model	Field	Model	% Error Model
1	84'	5743	8779	9099	3.64	3623	3480	-3.95	0.574	0.667	16.20
2	118.5'	6305	9638	9347	-3.02	4507	4794	6.37	0.574	0.556	-3.14
3	154'	5630	8002	8042	0.50	4643	4870	4.89	0.562	0.526	-6.41
4	197'	5908	7700	8097	5.16	4643	5260	13.29	0.574	0.538	-6.27
5	224'	5376	6557	6834	4.22	4189	4943	18.00	0.598	0.612	2.34

* Tension measured in pounds.

CHAPTER 9 - Effects on the Tailspar

The dynamics of the skyline can affect the loads which the tailspar will experience during a yarding operation. The effect will come not only from the fact that the skyline oscillates, creating a cyclical loading on the tailspar, but from the type of load that induces the oscillations in the skyline. The ways in which the computer model developed in this project can help predict the loads placed on a tailspar due to dynamic behavior of the skyline are discussed in the following paragraphs.

Resonance

Part of the information that is output from the computer model is the frequency at which the skyline oscillates. This frequency of oscillation for the skyline is also the frequency of the cyclical loading that the tailspar experiences. When the frequency of a loading matches the natural frequency of the structure on which the load is placed a phenomena known as resonance will occur. Resonance, also called dynamic magnification, is simply a magnification of the displacements, and stresses, of those which would occur under static conditions. Resonance is particularly dangerous because these displacements may continue to grow, if the frequency of the load continues to match the natural frequency of the structure, until failure of the structure occurs. However, once the dynamic load damps out, or the frequencies cease to match, the resonant behavior of the

structure will be eliminated.

In the field tests conducted for this project there was no evidence of resonance in the tailspar. For the tailspar used in this study, the fundamental frequency was 0.244 Hz and other natural frequencies that appeared rarely were 0.488 and 1.22 Hz. These frequencies did not match the frequency of the skyline oscillations which were on an average of 0.574 Hz. However, this does not mean that resonance could not occur in other tailspars. A longer skyline, having a lower natural frequency, could match the low frequency of this tailspar; also a stiffer tailspar, with a higher frequency could match the higher skyline frequencies. Or a combination of either of these things could result in frequencies of the tailspar matching the frequencies of the skyline and thus resonance of the tailspar.

The computer model can be useful in helping to avoid situations where resonance might occur. Used in combination with a modified version of the finite element program for tailspar analysis written by Ammeson, et al. [2], a version that would determine the natural frequencies of a tailspar (solve the eigenproblem), any matching of frequencies between the tailspar and skyline would be revealed before the actual occurrence in the field. With this type of information, resonance in the tailspar could be avoided by selecting another tailspar or changing the design of the skyline setup.

Forcing Function

Another way that the output from the computer model can be used is as input to the finite element model mentioned above [2]. The oscillations of the tension in the skyline, at the correct frequency, as determined by the model could be used as a forcing (loading) function in the finite element program. This would indicate how a tailspar responds under cyclical loading, perhaps revealing any magnification and/or fatigue related problems that might occur.

Dynamic Load Factor

One last way in which the dynamic behavior of the skyline affects the tailspar is not in the oscillations of the skyline but in the type of loading that causes the skyline oscillations. In the hang-up and eventual break out of the turn of logs, the skyline experiences a specific type of impulse load. An impulse load is simply a load that acts over a shorter period of time than a static load would. The type of impulse load developed by the hang-up/break out scenario is a ramp load, a load which builds up steadily and is suddenly reduced (Figure 31), the load being transferred through the skyline to the tailspar. When an impulse load acts on an elastic system there is a possibility of dynamic overshoot [27] described by the dynamic load factor, DLF [28]. The effect of the impulse load on the elastic system can be to increase the displacements, and the stresses, of the system over what

they would normally be in a static situation. Other possibilities are that the impulse load will decrease the displacements and load or not affect them at all. The factors that determine the influence the impulse load will have on an elastic system are the type of impulse load that occurs and the ratio of the duration of the impulse load, t, to the period of the elastic system, T. A spectrum of dynamic load factors for a simple oscillator [29] subjected to ramp loading as in Figure 31 is shown in Figure 32. A tailspar can be considered as a simple oscillator. The shaded portion of Figure 32 shows the range of dynamic load factors for the tailspar with a frequency of 0.244 Hz (T = 4.09 sec.) that resulted from the field experiments with the ramp loads that were placed on the skyline due to the hang-up/break out simulations. It should be noted that the shaded region of Figure 31 contains both the maximum, 1.23, and the minimum, 0.87, dynamic load factors that could occur for a simple oscillator. As the ratio t/T increases the dynamic load factor goes to one and the load behaves as a static load would. For other tailspars and ramp loads this spectrum could be used to determine the correct Dynamic Load Factor, with the appropriate dynamic load factor being used as a multiplier to the tensions output from the computer model for the skyline, or other tensions expected in the skyline, and the result would be the loads the tailspar would actually feel.

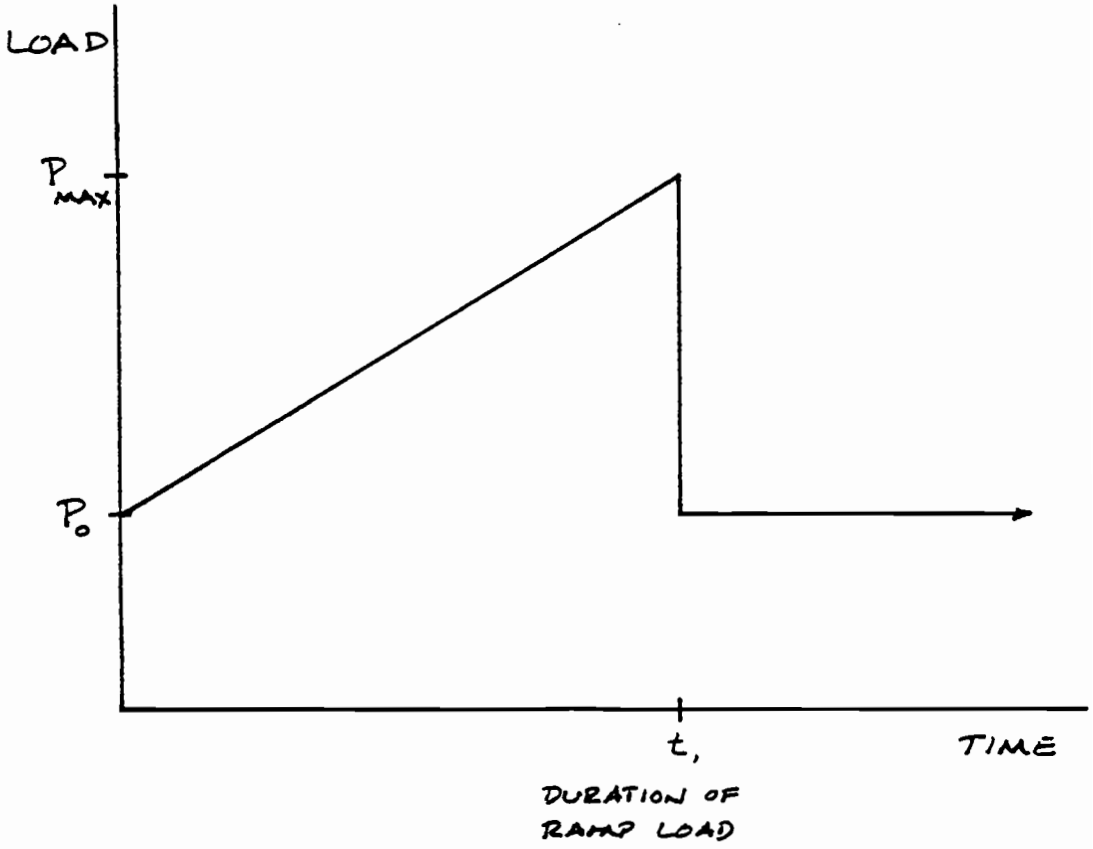

FIGURE 31 – Ramp Loading

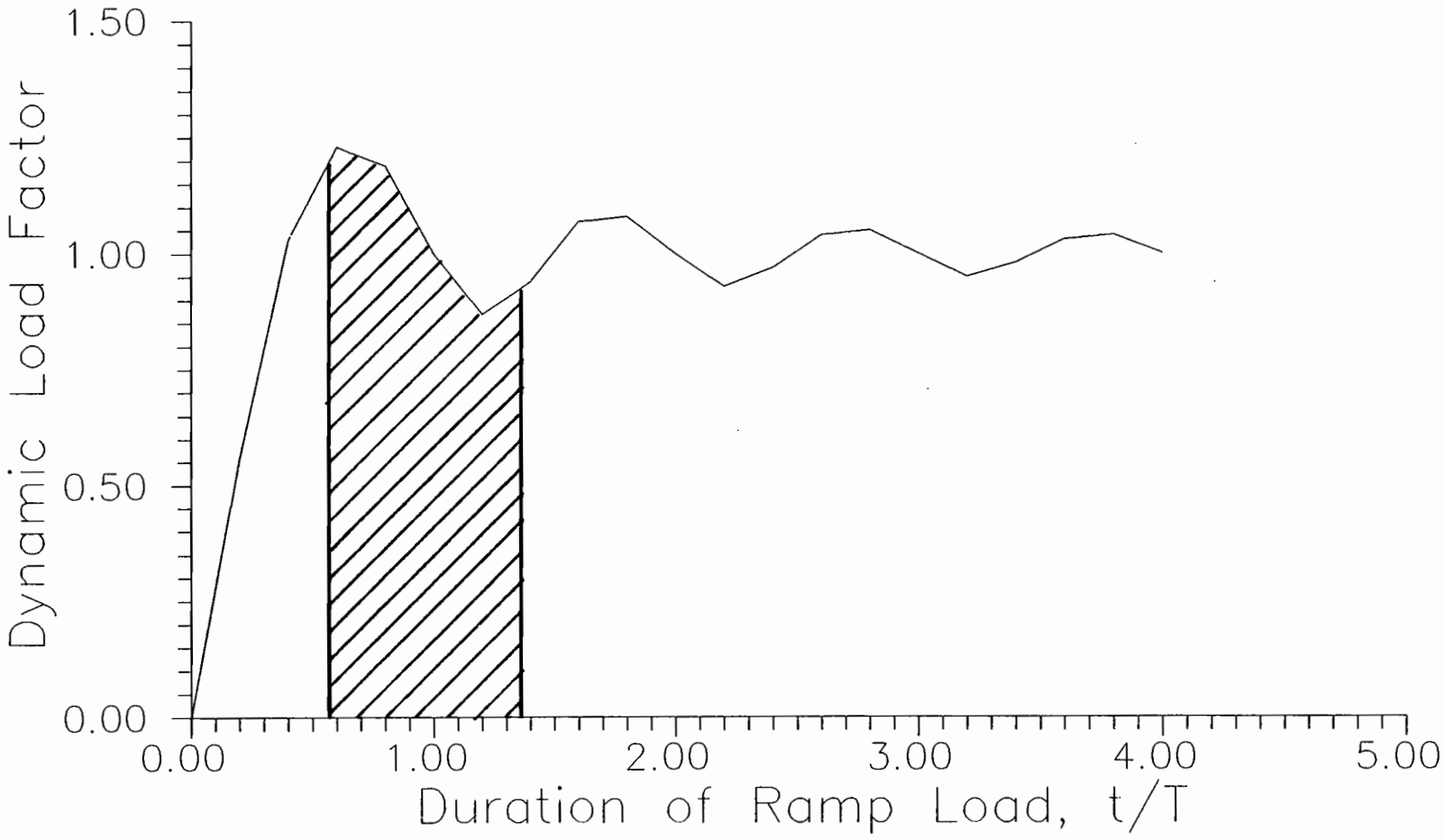

Figure 32 – Dynamic Overshoot, Impulse Load

CHAPTER 10 - Summary

The first portion of this paper entailed a study of the effects of incline on the frequencies of a taut cable (wire rope). An experimental investigation was undertaken to determine if incline does affect frequency and the results of these experiments were compared to theoretical frequencies. The results of the experimentation shows that inclining a cable at any angle from zero to 90 degrees has very little effect on the frequency of a taut cable and that the theoretical equation for horizontal cables can be used to calculate the frequency of an inclined cable.

The main body of this paper outlines a computer model developed to simulate the behavior of a cable logging system skyline. Utilizing this model the frequencies of a skyline with a log load can be extracted. The changes in tension of the skyline are also available, along with the displacements of the skyline if so desired, so that the changing dynamic loads on the tailspar can be determined. A finite difference approach was taken in this model utilizing a nine point implicit scheme which guarantees stability. The computer model appears to be reliable based on a comparison with 9 field tests. Matching the dynamic behavior of a skyline, particularly in a hang-up/break out situation, is by nature difficult given the unpredictability of the event. Each hang-up and break out

will be unique in its behavior even if it occurs at the same spot under the same circumstances. However, the computer model is within 16.2 percent error when compared to field experiments of a hang-up/ break out situation, for both the frequency and maximum tension calculated for the skyline.

The ultimate goal is to be able to determine if an increase in loading will occur on the tailspar due to the dynamics of the skyline. Based on the experimental work done it did not appear that any resonance in the tailspar did occur. Dynamic load factors did show themselves to be an important consideration, with both maximum, 1.23, and minimum, 0.87, values occurring. However, this is for just one specific tailspar. For other tailspars with longer skylines and different hang-up situations resonance could occur and different dynamic load factors would be considered.

Determining the dynamic behavior of a tailspar is a complicated and difficult procedure. Modeling the dynamic behavior of the skyline is one step in this procedure. However, this computer model of the skyline is not enough by itself to determine whether or not resonance might occur in the tailspar. Somehow the frequencies of the tailspar must be determined. A recommendation would be to modify the finite element program written by Ammeson, et al. [2] to include a routine to extract the natural

frequencies of the tailspar (solve the eigenproblem). When used together to compare the frequencies of the tailspar and skyline these two programs would be very powerful in determining whether or not resonance should be a concern for any given cable logging system. The dynamic loads placed on the skyline would also be available from the model produced in this study to be used as a forcing function type input to the finite element program. The influence of the dynamic load factor would need to be determined from an investigation into the types of impulse loads which occur on a skyline and the natural period of the tailspar, with a maximum value from the spectrum of a simple oscillator being 1.23.

If all of the above procedures were followed the dynamic behavior of any given tailspar, due to the dynamic skyline load, would be very apparent and any phenomena that might arise due to these dynamics, resonance, large dynamic load factors and fatigue, could be avoided.

BIBLIOGRAPHY

1. Pyles, Marvin R., Pugh, Edwin V., (1987). "Two-Dimensional Analysis of Logging Tail Spars", Forest Science, 33(4), 971-983.

2. Ammeson, James E., Pyles, Marvin R., Laursen, Harold I., (1988). "Three-Dimensional Analysis of Guyed Logging Spars", Computers and Structures, 29(6), 1095-1099.

3. Ammeson, James E., Pyles, Marvin R., Laursen, Harold I., (1988). "Dynamic Testing of a Guyed Logging Tailspar", Unpublished paper.

4. Foster-Miller, Inc., (1986). "Substitute Earth Anchoring System, Dynamic Analysis and Field Testing Report", U.S. Dept. of Agriculture, Report No. FSS-8266-R-048.

5. West, Harry H., Geschwindner, Louis F., Suhoski, Joseph E., (1975). "Natural Vibrations of Suspension Cables", J. Struct. Div., ASCE, 101(11), 2277-2291.

6. Henghold, William M., Russell, John J., Morgan, Joseph D., (1977). "Free Vibrations of Cables in Three Dimensions", J. Struct. Div., ASCE, 103(5), 1127-1136.

7. Irvine, Max H., (1981). "Cable Structures", The MIT Press, Cambridge, Mass.

8. Veletsos, Anestis S., Darbre, Georges R., (1983). "Free Vibration of Parabolic Cables", J. Struct. Eng., ASCE, 109(2), 503-519.

9. Triantafyllou, M. S., Grinfogel, L., (1986). "Natural Frequencies and Modes of Inclined Cables", J. Struct. Eng., ASCE, 112(1), 139-148.

10. Cook, Robert D., Malkus, David S., Plesha, Michael E., (1989). "Concepts and Applications of Fininte Element Analysis, 3rd Ed.", John Wiley and Sons, New York.

11. Leonard, John W., (1988). "Tension Structures", McGraw-Hill, New York.

12. Kaplan, Wilfred, (1981). "Advanced Mathematics for Engineers", Addison-Wesley, Reading, Mass.

13. Irvine, Max H., (1976). Discussion of "Natural Vibrations of Suspension Cables", by Harry H. West, Louis F. Geschwindner, Joseph E. Suhoski. J. Struct. Div., ASCE, 102(6), 1286-1288.

14. Irvine, Max H., (1978). "Free Vibrations of Inclined Cables", J. Struct. Div., ASCE, 104(2), 343-347.

15. _____, (1947). "Wire Rope", The Wire Rope Institute, Washington, D.C.

16. _____, (1969). "Steel Wire Handbook, Vol. 2", Wire Association, Inc., Branford, Conn.

17. Costello, George A., Phillips, James W., (1976). "Effective Modulus of Twisted Wire Cables", J. of the Engineering Mech. Div., ASCE, 100(2), 171-181.

18. Bendat, Julius S., Piersol, Allan G., (1971). "Random Data: Analysis and Measurement Procedures", Wiley-Interscience, New York.

19. _____, (1988). UnkelScope, Revision 3.05, M.I.T., Cambridge, Mass.

20. Devore, Jay L., (1982). "Probability and Statistics for Engineering and the Sciences", Brooks/Cole, Monterey, Cal.

21. Peyrot, A. H., Goulois, A. M., (1979). "Analysis of Cable Structures", Computers and Structures, 10(5), 805-813.

22. Jayaraman, H. B., Knudson, W. C., (1981). "A Curved Element for the Analysis of Cable Structures", Computers and Structures, 14(3-4), 325-333.

23. Tychonoff A. N., Samarski, A. A., (1959). "Differentialgleichungen der Mathematischen Physik", Veb Deutscher Verlag Der Wissenschaften, Berlin.

24. Ames, W. F., (1965). "Nonlinear Partial Differential Equations in Engineering", Academic Press, New York.

25. Atkinson, Kendall E., (1989). "An Introduction to Numerical Analysis, 2nd Ed.", John Wiley and Sons, New York.

26. Gere, James M., Timoshenko, Stephen P., (1984). "Mechanics of Materials, 2nd Ed.", Brooks/Cole, Monterey, Cal.

27. Craig Jr., Roy R., (1981). "Structural Dynamics, An Introduction to Computer Methods", John Wiley and Sons, New York.

28. Biggs, John M., (1964). "Introduction to Structural Dynamics", McGraw-Hill, New York.

29. Paz, Mario, (1986). "Microcomputer-Aided Engineering, Structural Dynamics", Van Nostrand Reinhold, New York.

APPENDICES

APPENDIX A

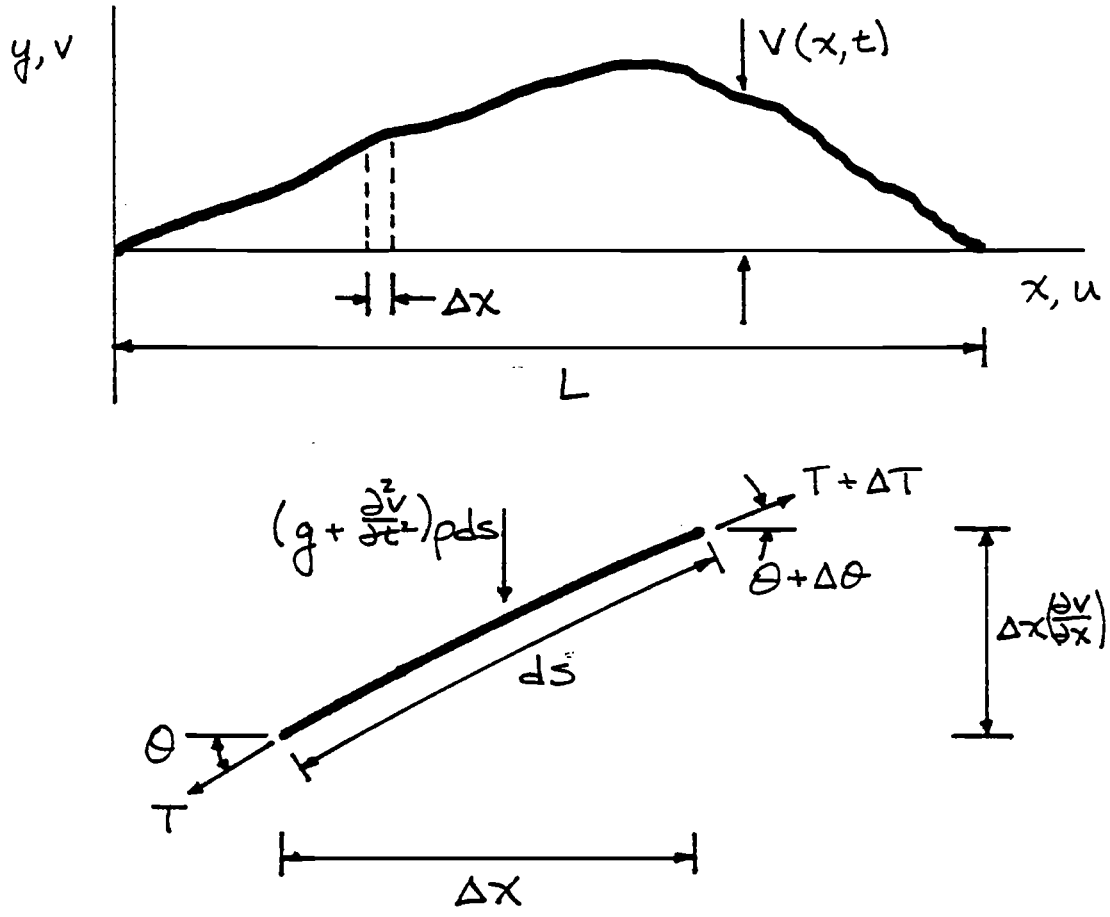

$$\Sigma F_x = 0$$

$$T(\cos\theta) = (T+\Delta T)(\cos(\theta+\Delta\theta))$$

FOR SMALL $\Delta\theta$:

$$\cos\theta \approx \cos(\theta+\Delta\theta)$$

$$\therefore \quad T(\cos\theta) = T(\cos\theta) + \Delta T(\cos\theta)$$

$$\Delta T = 0$$

APPENDIX A (cont.)

$$\Sigma F_y = 0$$

$$\left(g + \frac{\partial^2 v}{\partial t^2}\right)\rho\, ds = T\left(\sin(\theta+\Delta\theta) - \sin\theta\right)$$

FOR SMALL Δx:

$$ds \approx \sqrt{(\Delta x)^2 + \left(\Delta x \frac{\partial v}{\partial x}\right)^2} = \Delta x \sqrt{1+\left(\frac{\partial v}{\partial x}\right)^2}$$

$$\left(g + \frac{\partial^2 v}{\partial t^2}\right)\left(\Delta x \sqrt{1+\left(\frac{\partial v}{\partial x}\right)^2}\right) = \frac{T}{\rho}\left(\tan(\theta+\Delta\theta) - \tan\theta\right)\cos\theta$$

$$\left(g + \frac{\partial^2 v}{\partial t^2}\right)\left(\Delta x \sqrt{1+\left(\frac{\partial v}{\partial x}\right)^2}\right) = \frac{T}{\rho}\left(\frac{\partial v}{\partial x}(x+\Delta x, t) - \frac{\partial v}{\partial x}(x,t)\right)\cos\theta$$

$$\left(g + \frac{\partial^2 v}{\partial t^2}\right)\left(\Delta x \sqrt{1+\left(\frac{\partial v}{\partial x}\right)^2}\right) = \frac{T(\Delta x)}{\rho}\left(\frac{\partial^2 v}{\partial x^2}(p,t)\right)\cos\theta$$

WHERE $\quad x < p < (x+\Delta x)$

$$\frac{\partial^2 v}{\partial t^2} = \frac{T}{\rho}\left(\frac{\partial^2 v}{\partial x^2}\right)\left(\frac{\cos\theta}{\sqrt{1+\left(\frac{\partial v}{\partial x}\right)^2}}\right) - g \qquad \text{(NON-LINEAR)}$$

LINEAR ASSUMPTIONS:

1) $\cos\theta \approx 1$
2) $\frac{\partial v}{\partial x} \approx 0$
3) T IS CONSTANT
4) g USUALLY NEGLECTED

$$T\frac{\partial^2 v}{\partial x^2} = \rho\frac{\partial^2 v}{\partial t^2}$$

APPENDIX B

EQUATION OF MOTION:

$$T\frac{\partial^2 v(x,t)}{\partial x^2} = \rho \frac{\partial^2 v(x,t)}{\partial t^2}$$

BY SEPARATION OF VARIABLES:

$$V(x,t) = G(x)F(t)$$

FOR A CABLE OF LENGTH L:

$$G(x) = C_1 \cos\left(\frac{n\pi x}{L}\right) + C_2 \sin\left(\frac{n\pi x}{L}\right)$$

$$F(t) = e^{i\omega t}$$

FROM BOUNDARY CONDITIONS, $V(0,t) = V(L,t) = 0$

$$C_1 = 0 \quad , \quad n = 1, 2, 3, 4, \ldots\ldots$$

$$\frac{\partial^2 v(x,t)}{\partial x^2} = -e^{i\omega t}\left\{C_2\left(\frac{n\pi}{L}\right)^2 \sin\left(\frac{n\pi x}{L}\right)\right\}$$

$$\frac{\partial^2 v(x,t)}{\partial t^2} = -\omega^2 e^{i\omega t}\left\{C_2 \sin\left(\frac{n\pi x}{L}\right)\right\}$$

$$T\left\{-e^{i\omega t} C_2 \left(\frac{n\pi}{L}\right)^2 \sin\left(\frac{n\pi x}{L}\right)\right\} = \rho\left\{-\omega^2 e^{i\omega t} C_2 \sin\left(\frac{n\pi x}{L}\right)\right\}$$

$$\omega^2 = \frac{T}{\rho}\left(\frac{n\pi}{L}\right)^2$$

$$\omega = \frac{n\pi}{L}\sqrt{\frac{T}{\rho}}$$

$$\omega = 2\pi f$$

$$f_n = \frac{n}{2L}\sqrt{\frac{T}{\rho}}$$

APPENDIX C

DIVIDED DIFFERENCES

x	$V(x, t_j)$	$\frac{\partial V(x,t_j)}{\partial x}$	$\frac{1}{2}\left(\frac{\partial^2 V(x,t_j)}{\partial x^2}\right)$
x_{i-1}	$V(x_{i-1}, t_j)$		
		$\frac{V_{i,j} - V_{i-1,j}}{\Delta x}$	
x_i	$V(x_i, t_j)$		$\frac{\frac{V_{i+1,j} - V_{i,j}}{\Delta x} - \frac{V_{i,j} - V_{i-1,j}}{\Delta x}}{2\Delta x}$
		$\frac{V_{i+1,j} - V_{i,j}}{\Delta x}$	
x_{i+1}	$V(x_{i+1}, t_j)$		

t	$V(x_i, t)$	$\frac{\partial V(x_i,t)}{\partial t}$	$\frac{1}{2}\left(\frac{\partial^2 V(x_i,t)}{\partial t^2}\right)$
t_{j-1}	$V(x_i, t_{j-1})$		
		$\frac{V_{i,j} - V_{i,j-1}}{\Delta t}$	
t_j	$V(x_i, t_j)$		$\frac{\frac{V_{i,j+1} - V_{i,j}}{\Delta t} - \frac{V_{i,j} - V_{i,j-1}}{\Delta t}}{2\Delta t}$
		$\frac{V_{i,j+1} - V_{i,j}}{\Delta t}$	
t_{j+1}	$V(x_i, t_{j+1})$		

APPENDIX D

FREE BODY DIAGRAM OF POINT MASS:

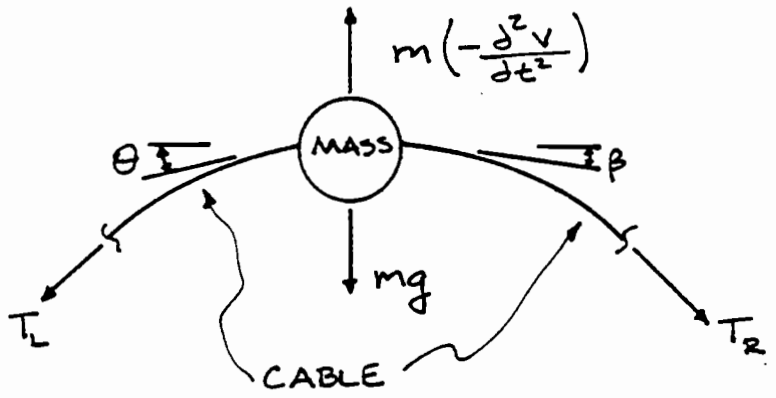

$$\Sigma F_V = 0$$

$$0 = m\left(-\frac{d^2V}{dt^2}\right) - mg - T_L \sin\theta - T_R \sin\beta$$

$$m\left(\frac{d^2V}{dt^2}\right) = -mg - T_L \cos\theta \tan\theta - T_R \cos\beta \tan\beta$$

$$\frac{d^2V}{dt^2} = \frac{V_{i,j-1} - 2V_{i,j} + V_{i,j+1}}{2(\Delta t)^2}$$

$$m\left(\frac{V_{i,j-1} - 2V_{i,j} + V_{i,j+1}}{2(\Delta t)^2}\right) = -mg - T_L \cos\theta \tan\theta - T_R \cos\beta \tan\beta$$

$$\frac{V_{i,j-1} - 2V_{i,j} + V_{i,j+1}}{2(\Delta t)^2} = -\frac{T_L}{m}\cos\theta\tan\theta - \frac{T_R}{m}\cos\beta\tan\beta - g$$

$$V_{i,j+1} = -\frac{2(\Delta t)^2}{m}\left(T_L \cos\theta\tan\theta + T_R \cos\beta\tan\beta\right) - 2g - V_{i,j-1} + 2V_{i,j}$$

APPENDIX E

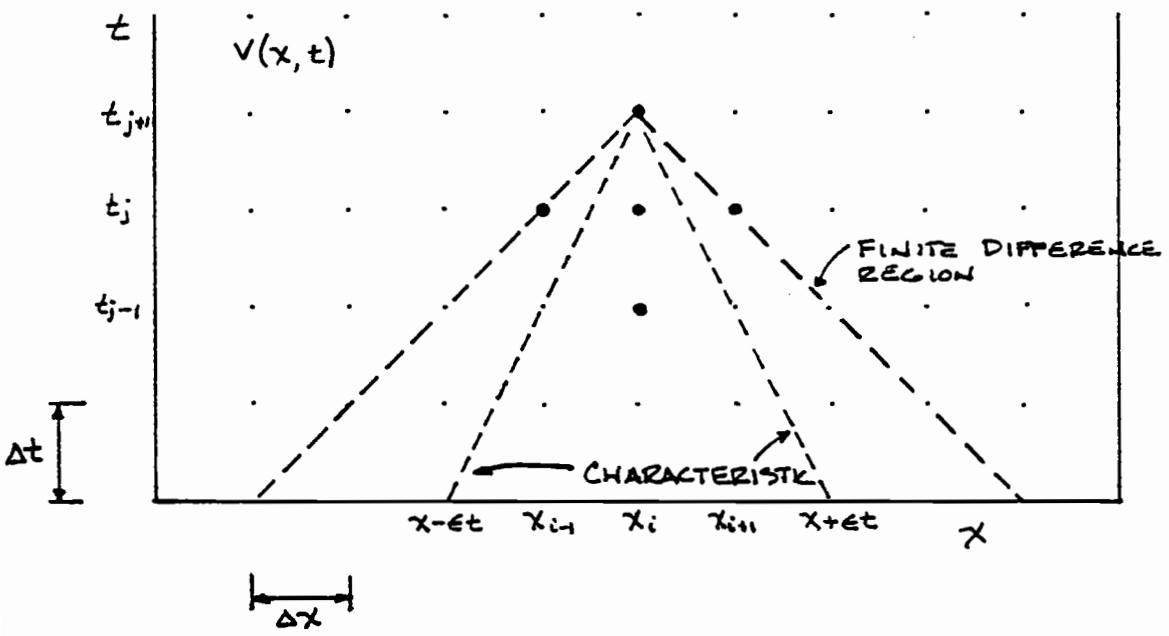

$$T\frac{\partial^2 V}{\partial x^2} = \rho\frac{\partial^2 V}{\partial t^2} \quad \text{or} \quad \epsilon^2\frac{\partial^2 V}{\partial x^2} = \frac{\partial^2 V}{\partial t^2}$$

$$\text{WHERE} \quad \epsilon^2 = \frac{T}{\rho}$$

$$\text{SLOPE OF CHARACTERISTIC} = \pm\frac{1}{\epsilon}$$

FOR STABILITY, REGION OF CHARACTERISTIC MUST BE UNDER THE FINITE DIFFERENCE REGION:

$$\frac{\Delta t}{\Delta x} \le \frac{1}{\epsilon}$$

$$\frac{\Delta t}{\Delta x}\left(\frac{\sqrt{T}}{\sqrt{\rho}}\right) \le 1 \quad , \quad \epsilon = \frac{\sqrt{T}}{\sqrt{\rho}}$$

$$\frac{(\Delta t)^2}{(\Delta x)^2}\left(\frac{T}{\rho}\right) \le 1 \quad , \quad \lambda = \frac{(\Delta t)^2}{(\Delta x)^2}\left(\frac{T}{\rho}\right)$$

$$\therefore \lambda \le 1$$

APPENDIX F

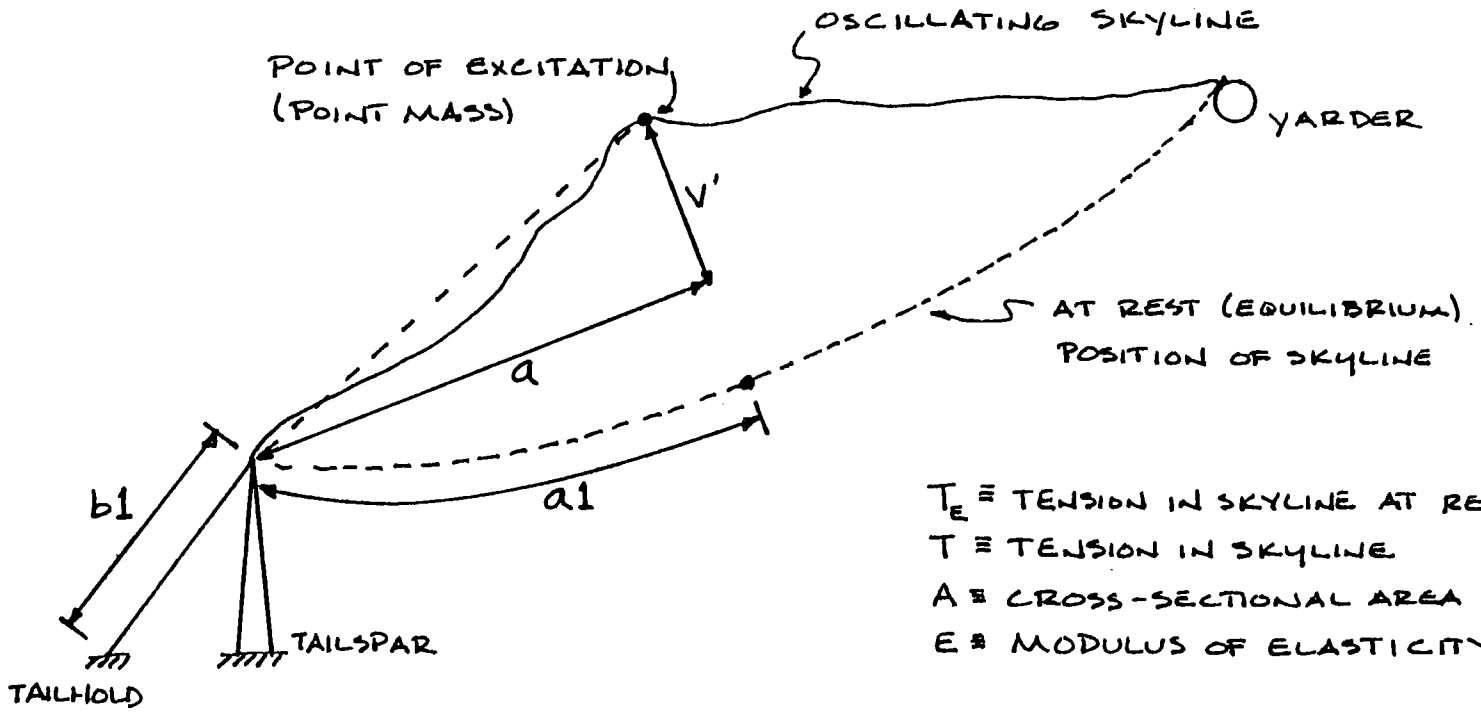

$$\Delta T = \left(\frac{\sqrt{a^2 + v'^2} - a1}{(a1 + b1)} \right) \times A \times E$$

$$T = T_E + \Delta T$$

APPENDIX G

```
{************SKYLINE DYNAMICS PROGRAM************}


PROGRAM SkylineDynamics;
USES Crt,Printer;
    TYPE
    matrix=ARRAY[0..2000,0..4] OF real;
    VAR
    m,ma,n:integer;
    a,a1,ar,b,b1,c,c1,d,dt,dx,E,g,H,H1,H2,
    lam,p,s,t,w,w1,w2:real;
    v:matrix;
    f:text;


PROCEDURE clear;
BEGIN
    TextBackground(white);
    ClrScr;
END;
```

APPENDIX G (cont.)

```
PROCEDURE input;
BEGIN
    writeln('Enter distance from tailspar
     to yarder:');
    read(b);
    writeln('Enter length of skyline from
     tailspar to tailhold:');
    read(b1);
    writeln('Enter diameter of skyline:');
    read(ar);
    ar:=0.395*sqr(ar);                              {1}
    writeln('Enter modulus of elasticity:');
    read(E);
    writeln('Enter initial tension in skyline:');
    read(H);
    writeln('Enter weight per foot of the
     skyline:');
    read(p);
    writeln('Enter weight of carriage:');
    read(w);
    writeln('Enter load placed on skyline
     by logs:');
    read(w1);
    w2:=w+w1;                                       {2}
    writeln('Enter magnitude for acceleration
     of gravity:');
    read(g);
    writeln('Enter size of element along the
     skyline:');
    read(dx);
    writeln('Enter size of time step:');
    read(dt);
    writeln('Enter length of time for analysis:');
    read(t);
    writeln('Enter distance from tailspar to
     hang-up:');
    read(a);
    writeln('Enter amount of displacement created
     by hang-up:');
    read(d);
    lam:=(1/(p/g))*sqr(dt/dx);                      {3}
    writeln('  ');
    writeln('Lambda = ',H*lam:5:3);
END;
```

APPENDIX G (cont.)

```
PROCEDURE Initial;
    VAR
    HH,q,r,slp:real;
    i,j:integer;
BEGIN
    q:=b/dx;                                          {4}
    m:=trunc(q);
    q:=t/dt;                                          {5}
    n:=trunc(q);
    q:=a/dx;                                          {6}
    ma:=trunc(q);
    c:=b-a;                                           {7}
    FOR j:=0 TO 4 DO
       BEGIN
          FOR i:=0 TO m DO
          BEGIN
          v[i,j]:=0.0;
          v[i,j]:=0.0;
          END;
       END;
    r:=w2*c/b+p*b/2;                                  {8}
    HH:=sqrt(sqr(H)-sqr(r));                          {9}
    FOR i:=1 TO ma DO
       v[i,4]:=-(r*i*dx-(p*sqr(i*dx))/2)/HH;          {10}
    FOR i:=ma+1 TO m-1 DO
       v[i,4]:=-(r*i*dx-(p*sqr(i*dx))/2-
         w2*(i*dx-a))/HH;
    slp:=d/a;                                         {11}
    FOR i:=0 TO ma DO                                 {12}
       BEGIN
       v[i,1]:=i*slp*dx;
       v[i,2]:=v[i,1];
       v[i,3]:=v[i,4]+v[i,1];
       END;
    a1:=0.0;
    q:=0.0;
    FOR i:=0 TO ma-1 DO                               {13}
       BEGIN
       a1:=sqrt(sqr(v[i+1,4]-v[i,4])+sqr(dx))+a1;
       q:=sqrt(sqr(v[i+1,3]-v[i,3])+sqr(dx))+q;
       END;
    H1:=H+((q-a1)/(a1+b1))*ar*E;                      {14}
    slp:=-d/c;                                        {15}
    FOR i:=ma+1 TO m DO                               {16}
       BEGIN
       v[i,1]:=(d+(i-ma)*slp*dx);
       v[i,2]:=v[i,1];
       v[i,3]:=v[i,4]+v[i,1];
       END;
```

APPENDIX G (cont.)

```
    c1:=0.0;
    q:=0.0;
    FOR i:=ma TO m-1 DO                                    {17}
       BEGIN
       c1:=sqrt(sqr(v[i+1,4]-v[i,4])+sqr(dx))+c1;
       q:=sqrt(sqr(v[i+1,3]-v[i,3])+sqr(dx))+q;
       END;
    H2:=H+((q-c1)/c1)*ar*E;                                {18}
    s:=0.0;
    writeln(f,'       Time ',' Tension');
    writeln(f,s:12:3,H1:12:3);                             {19}
END;


PROCEDURE Slopes;                                          {20}
    VAR
    i:integer;
BEGIN
    v[0,0]:=(1/dx)*v[1,2];
    v[m,0]:=-(1/dx)*v[m-1,2];
    FOR i:=1 TO m-1 DO
       BEGIN
       v[i,0]:=(1/(2*dx))*(v[i+1,2]-v[i-1,2]);
       END;
END;


PROCEDURE Massdispl;                                       {21}
    VAR
    q,beta,theta:real;
BEGIN
    theta:=arctan(((v[ma,2]+v[ma,4])-
      (v[ma-1,2]+v[ma-1,4]))/dx);                          {22}
    theta:=cos(theta);
    beta:=arctan(((v[ma,2]+v[ma,4])-
      (v[ma+1,2]+v[ma+1,4]))/dx);                          {23}
    beta:=cos(theta);
    q:=((2*H1*sqr(dt))/w2)*theta*((v[ma-1,2]+
      v[ma-1,4])-(v[ma,2]+v[ma,4]))/dx+
      ((2*H2*sqr(dt))/w2)*beta*((v[ma+1,2]+
      v[ma+1,4])-(v[ma,2]+v[ma,4]))/dx-
      2*sqr(dt)*(g);                                       {24}
    v[ma,3]:=q+2*v[ma,2]-v[ma,1];                          {25}
END;
```

APPENDIX G (cont.)

```
PROCEDURE GaussL;
    VAR
    i:integer;
    tri:matrix;
    q:real;
BEGIN
    FOR i:=0 TO ma-1 DO
       BEGIN
       tri[i,0]:=arctan(v[i,0]);                    {26}
       tri[i,0]:=cos(tri[i,0]);
       v[i,0]:=tri[i,0]/(sqrt(1+sqr(v[i,0])));{27}
       END;
    v[ma,0]:=(v[ma,3]-v[ma-1,2])/dx;                {28}
    tri[ma,0]:=arctan(v[ma,0]);
    tri[ma,0]:=cos(tri[ma,0]);
    v[ma,0]:=tri[ma,0]/(sqrt(1+sqr(v[ma,0])));
    tri[0,0]:=-(1+(lam/2)*H1*v[0,0])*v[0,1]+    {29}
      (2-lam*H1*v[0,0])*v[0,2];
    FOR i:=1 TO ma-1 DO                             {30}
       BEGIN
       q:=-(lam/2)*H1*v[i,0]*v[i,1]-lam*H1*
         v[i,0]*v[i,2]+(lam/2)*H1*v[i,0]*
         (v[i-1,2]+v[i+1,2])+(lam/4)*
         H1*v[i,0]*(v[i-1,1]+v[i+1,1]);
       tri[i,0]:=-v[i,1]+2*v[i,2]+q;
       END;
    tri[ma,0]:=v[ma,3];                             {31}
    FOR i:=0 TO ma-1 DO                             {32}
       BEGIN
       tri[i,1]:= (-lam/4)*H1*v[i,0];
       tri[i,2]:= 1+(lam/2)*H1*v[i,0];
       tri[i,3]:= (-lam/4)*H1*v[i,0];
       END;
    tri[0,1]:=0.0;                                  {33}
    tri[ma,3]:=0.0;
    tri[0,3]:=0.0;
    tri[ma,1]:=0.0;
    tri[ma,2]:=1.0;
    tri[0,0]:=tri[0,0]/tri[0,2];                    {34}
    tri[0,3]:=tri[0,3]/tri[0,2];
    tri[0,2]:=1.0;
    FOR i:=1 TO ma-1 DO                             {35}
       BEGIN
       tri[i,0]:=tri[i,0]-tri[i,1]*tri[i-1,0];
       tri[i,2]:=tri[i,2]-tri[i,1]*tri[i-1,3];
       tri[i,1]:=0.0;
       tri[i,0]:=tri[i,0]/tri[i,2];
       tri[i,3]:=tri[i,3]/tri[i,2];
       tri[i,2]:=1.0;
       END;
```

APPENDIX G (cont.)

```
    v[ma,3]:=tri[ma,0];                                    {36}
    FOR i:= ma-1 DOWNTO 0 DO
       BEGIN
       v[i,3]:=tri[i,0]-tri[i,3]*v[i+1,3];
       END;
END;


PROCEDURE GaussR;
    VAR
    i:integer;
    tri:matrix;
    q:real;
BEGIN
    FOR i:=ma+1 TO m DO
       BEGIN
       tri[i,0]:=arctan(v[i,0]);
       tri[i,0]:=cos(tri[i,0]);
       v[i,0]:=tri[i,0]/(sqrt(1+sqr(v[i,0])));
       END;
    v[ma,0]:=(v[ma+1,2]-v[ma,3])/dx;
    tri[ma,0]:=arctan(v[ma,0]);
    tri[ma,0]:=cos(tri[ma,0]);
    v[ma,0]:=tri[ma,0]/(sqrt(1+sqr(v[ma,0])));
    {Calculation of b, in Ax=b matrix equation}
    tri[ma,0]:=v[ma,3];
    FOR i:=ma+1 TO m-1 DO
       BEGIN
       q:=-(lam/2)*H2*v[i,0]*v[i,1]-lam*H2*
         v[i,0]*v[i,2]+(lam/2)*H2*v[i,0]*
         (v[i-1,2]+v[i+1,2])+(lam/4)*
         H2*v[i,0]*(v[i-1,1]+v[i+1,1]);
       tri[i,0]:=-v[i,1]+2*v[i,2]+q;
       END;
    tri[m,0]:=-(1+(lam/2)*H2*v[m,0])*v[m,1]+
      (2-lam*H2*v[m,0])*v[m,2];
    FOR i:=ma+1 TO m DO
       BEGIN
       tri[i,1]:= (-lam/4)*H2*v[i,0];
       tri[i,2]:= 1+(lam/2)*H2*v[i,0];
       tri[i,3]:= (-lam/4)*H2*v[i,0];
       END;
    tri[ma,1]:=0.0;
    tri[m,3]:=0.0;
    tri[ma,3]:=0.0;
    tri[m,1]:=0.0;
    tri[ma,2]:=1.0;
    tri[ma,0]:=tri[ma,0]/tri[ma,2];
    tri[ma,3]:=tri[ma,3]/tri[ma,2];
    tri[ma,2]:=1.0;
```

APPENDIX G (cont.)

```
    FOR i:=ma+1 TO m DO
       BEGIN
       tri[i,0]:=tri[i,0]-tri[i,1]*tri[i-1,0];
       tri[i,2]:=tri[i,2]-tri[i,1]*tri[i-1,3];
       tri[i,1]:=0.0;
       tri[i,0]:=tri[i,0]/tri[i,2];
       tri[i,3]:=tri[i,3]/tri[i,2];
       tri[i,2]:=1.0;
       END;
    v[m,3]:=tri[m,0];
    FOR i:= m-1 DOWNTO ma DO
       BEGIN
       v[i,3]:=tri[i,0]-tri[i,3]*v[i+1,3];
       END;
END;


PROCEDURE Mainroutine;
    VAR
    i,k:integer;
    q:real;
    BEGIN
    INITIAL;
    w2:=w2/g;                                          {37}
    p:=p/g;                                            {38}
    FOR k:=1 TO n-1 DO                                 {39}
       BEGIN
       SLOPES;
       MASSDISPL;
       GAUSSL;
       GAUSSR;
       s:=(k)*dt;                                      {40}
       writeln(k);
       q:=sqrt(sqr(a)+sqr(v[ma,3]+v[ma,4]));           {41}
       H1:=H+((q-a1)/(a1+b1))*ar*E;                    {42}
       q:=sqrt(sqr(c)+sqr(v[ma,3]+v[ma,4]));           {43}
       H2:=H+((q-c1)/c1)*ar*E;                         {44}
       FOR i:=0 TO m DO                                {45}
          BEGIN
          v[i,1]:=v[i,2];
          v[i,2]:=v[i,3];
          END;
       writeln(f,s:12:3,H1:12:3);                      {46}
       END;
END;
```

APPENDIX G (cont.)

```
BEGIN{Main Program}
 {$M 65520,0,655360}
 clear;
 input;
 assign(f, 'filename.ext');                    {47}
 rewrite(f);
 mainroutine;
 close(f);
END.


{************************************************}
{ This program is a non-linear finite difference }
{  model for dynamic cable displacements.  Gauss }
{  elimination is used to solve for displacements}
{  using a 9 point scheme.                       }
{ The variables are defined as follows:          }
{ a=distance from tailspar to hang-up            }
{ a1=length of skyline from tailspar to hang-up  }
{ ar=area of skyline cross section               }
{ b=distance from tailspar to yarder             }
{ b1=length of skyline from tailspar to tailhold }
{ c=distance from yarder to hang-up              }
{ c1=length of skyline from yarder to hang-up    }
{ d=amount of initial displacement created by    }
{   hang-up                                      }
{ dt=size of time step                           }
{ dx=size of element along length of skyline     }
{ E=Modulus of Elasticity                        }
{ g=magnitude for acceleration of gravity        }
{ H=initial skyline tension                      }
{ HH=horizontal component of skyline tension     }
{ H1=tension in skyline at tail spar             }
{ H2=tension in skyline at yarder                }
{ lam=Lambda, the stability factor, usually equal}
{     to (H/p)*sqr(dt/dx), but in this program   }
{     the tension is taken out as a variable.    }
{ m=number of elements along skyline             }
{ ma=number of elements from tailspar to point of}
{    initial displacements                       }
{ n=number of time steps                         }
{ p=weight, then mass per linear foot of skyline }
{ q=dumby variable                               }
{ r=vertical reaction at tailspar                }
{ s=equals current time in the analysis          }
{ slp=slope of a skyline segment                 }
{ t=end time for analysis                        }
```

APPENDIX G (cont.)

```
{ tri=tri-diagonal matrix used in Gauss          }
{     elimination. The first column is the "b"   }
{     column martix, the next 3 columns are the  }
{     "x" matrix in the matrix equation Ax=b.    }
{ v=displacement of skyline, a function of x and }
{   time.  The v matrix has 5 columns:  The first}
{   column is the non-linear multiplier, the next}
{   3 columns are the displacements at time steps}
{   k-1, k, k+1 respectively.  The last column is}
{   the original position of the cable at        }
{   equilibrium.                                 }
{ w=weight of carriage                           }
{ w1=weight of log load                          }
{ w2=weight of carriage and log load             }
{                                                }
{                                                }
{The following is a commentary on the steps and  }
{procedures contained in this program.  Each     }
{numbered comment here corresponds to the line or}
{procedure highlighted by that number.           }
{                                                }
{ 1)  Calculate cross-sectional area of wire rope}
{                                                }
{ 2)  Sum weight of carriage and log load        }
{                                                }
{ 3)  Calculate lambda                           }
{                                                }
{ 4)  Determine number of elements along skyline }
{                                                }
{ 5)  Determine number of time steps             }
{                                                }
{ 6)  Determine number of elements between the   }
{     tailspar and hang-up                       }
{                                                }
{ 7)  Calculate distance from yarder to hang-up  }
{                                                }
{ 8)  Calculate vertical reaction at tailspar    }
{                                                }
{ 9)  Calculate horizontal component of skyline  }
{     tension                                    }
{                                                }
{ 10)  These two loops determine the initial     }
{      position of the cable due to its own      }
{      weight, a parabolic approximation         }
{                                                }
{ 11)  Slope of skyline, between tailspar and    }
{      hang-up, due to vertical deflection       }
{      created by hang-up                        }
```

APPENDIX G (cont.)

```
{ 12)  This loop superimposes the deflections due}
{      to the cable weight and hang-up to get the}
{      position of the skyline as the turn of    }
{      logs breaks loose from the hang-up        }
{                                                }
{ 13)  This loop calculates the length of the    }
{      skyline, between tailspar and hang-up,    }
{      when displaced under its own weight and   }
{      then when carriage and log load are placed}
{      on the skyline                            }
{                                                }
{ 14)  Calculates increase in tension of the     }
{      skyline, between tailspar and hang-up, due}
{      to hang-up displacement                   }
{                                                }
{ 15)  Same as {11}, except between hang-up and  }
{      yarder                                    }
{                                                }
{ 16)  Same as {12}, except between hang-up and  }
{      yarder                                    }
{                                                }
{ 17)  Same as {13}, except between hang-up and  }
{      yarder                                    }
{                                                }
{ 18)  Same as {14}, except between hang-up and  }
{      yarder                                    }
{                                                }
{ 19)  Outputs time step and skyline tension to  }
{      file                                      }
{                                                }
{ 20)  This loop calculates the slope of the     }
{      skyline at each node                      }
{                                                }
{ 21)  This loop determines the position of the  }
{      point mass                                }
{                                                }
{ 22)  Determines the angle of the skyline as it }
{      goes into the carriage from the tailspar  }
{                                                }
{ 23)  Determines the angle of the skyline as it }
{      goes into the carriage from the yarder    }
{                                                }
{ 24)  Intermediate step in summing forces on the}
{      point mass, transverse to the skyline     }
{                                                }
{ 25)  Final summation of forces on the point    }
{      mass, transverse to the skyline, including}
{      a finite difference treatment for the     }
{      acceleration of the point mass to         }
{      the position of the point mass            }
```

APPENDIX G (cont.)

```
{ NOTE:  Procedure GaussL determines the          }
{        displacement of the skyline between the  }
{        tailspar and hang-up, using Gauss        }
{        elimination.  GaussR is an identical     }
{        procedure except it determines the       }
{        displacements of the skyline between the }
{        hang-up and yarder.                      }
{                                                 }
{ 26)  Calculates the cosine of the skyline at    }
{      each node                                  }
{                                                 }
{ 27)  Determines the nonlinear multiplier for    }
{      wave equation                              }
{                                                 }
{ 28)  Determines the cosine of the skyline and   }
{      nonlinear multiplier at the carriage       }
{                                                 }
{ 29)  Determines first term of the "b" vector in }
{      the Ax=b matrix equation                   }
{                                                 }
{ 30)  Determines the remaining terms of the "b"  }
{      vector, except at the carriage             }
{                                                 }
{ 31)  Determines the last term of the "b" vector }
{      at the carriage                            }
{                                                 }
{ 32)  This loop creates the tri-diagonal "A"     }
{      and places it in a three column matrix     }
{                                                 }
{ 33)  These five steps corrects the "A" matrix   }
{      for the terms that would not exist in the  }
{      tri-diagonal matrix and the fifth step     }
{      reflects the boundary at the carriage      }
{                                                 }
{ 34)  First steps in forming the upper           }
{      triangular matrix, with main diagonal      }
{      equal to 1, required for Gauss elimination }
{                                                 }
{ 35)  This loop completes the upper triangular   }
{      matrix                                     }
{                                                 }
{ 36)  Back substitution to solve for the "x"     }
{      matrix, which in this program is the       }
{      dispacements of the skyline                }
{                                                 }
{ 37)  Determines the mass of the carriage and    }
{      turn of logs                               }
{                                                 }
{ 38)  Determines the linear mass of the skyline  }
```

APPENDIX G (cont.)

```
{ 39)  Loop which is run at each time step       }
{                                                }
{ 40)  Increments the number of the time step    }
{                                                }
{ 41)  Calculates the change in length of the    }
{      skyline, between the tailspar and hang-up,}
{      due to the dynamic displacements          }
{                                                }
{ 42)  Calculates the tension in the skyline     }
{      between the tailspar and hang-up          }
{                                                }
{ 43)  Same as {41}, except between hang-up and  }
{      yarder                                    }
{                                                }
{ 44)  Same as {42}, except between hang-up and  }
{      yarder                                    }
{                                                }
{ 45)  Shifts displacement values in the v matrix}
{                                                }
{ 46)  Outputs time step and skyline tension to  }
{      file                                      }
{                                                }
{ 47)  Assigns an output file for program output }
{************************************************}
```